

# Flume Experiments on the Transport of a Coarse Sand

---

GEOLOGICAL SURVEY PROFESSIONAL PAPER 562-B



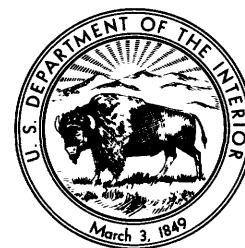
# Flume Experiments on the Transport of a Coarse Sand

*By* GARNETT P. WILLIAMS

SEDIMENT TRANSPORT IN ALLUVIAL CHANNELS

---

GEOLOGICAL SURVEY PROFESSIONAL PAPER 562-B



---

UNITED STATES GOVERNMENT PRINTING OFFICE, WASHINGTON : 1967

**UNITED STATES DEPARTMENT OF THE INTERIOR**

**STEWART L. UDALL, *Secretary***

**GEOLOGICAL SURVEY**

**William T. Pecora, *Director***

## CONTENTS

	Page		Page
Symbols.....	iv	Results.....	B6
Abstract.....	B1	General.....	6
Introduction.....	1	Sediment-transport rates.....	6
Equipment and application.....	2	Relations of variables.....	13
Flume.....	2	Surface velocity.....	16
Water circuit and discharge measurement.....	2	Comparison with data of Gilbert and Murphy.....	18
Sediment infeed.....	2	Bed forms.....	20
Sediment-transport measurement.....	3	Interrelations between characteristics.....	22
Sediment.....	3	Characteristics related to fluid flow strength.....	23
Procedure.....	3	Characteristics related to sediment-transport rates.....	25
Initiation of runs and attainment of equilibrium conditions.....	3	Conclusions.....	28
Measurements.....	5	Description of bed configuration, by run.....	28
		References.....	30

## ILLUSTRATIONS

FIGURES 1-16. Graphs:		Page
1. Size analysis of sand.....		B3
2. Power versus transport relation.....		9
3. Shear ( $\gamma DS$ ) versus transport relation.....		9
4. Shear ( $\gamma RS$ ) versus transport relation.....		10
5. Mean velocity versus transport relation.....		10
6. Regime bed factor versus transport relation.....		11
7. Transport relations adjusted for flume wall drag (Einstein method).....		14
8. Discharge versus transport relation.....		14
9. Slope versus transport relation.....		15
10. Relations of slope to discharge and mean velocity.....		16
11. Surface velocity versus transport relation.....		17
12. $V/V_s$ relation for various depths.....		17
13. Relations of surface velocity to slope and discharge.....		18
14. Comparison of stream power versus transport relations with data of Gilbert and Murphy.....		19
15. Comparison of shear versus transport relation with data of Gilbert and Murphy.....		19
16. Mean velocity versus shear ( $DS$ ) relations compared with data of Gilbert and Murphy.....		20
17. Sketch showing pattern of typical meandering scars.....		21
18-25. Graphs:		
18. Variation in bed-form height with travel velocity.....		23
19. Variation in bed-form wavelength with travel velocity.....		24
20. Bed-form height versus measures of flow strength.....		25
21. Bed-form wavelengths versus measures of flow strength.....		26
22. Bed-form velocity versus measures of flow strength.....		26
23. Relation of bed-form height to sediment-transport rate.....		27
24. Variation in bed-form velocity with sediment-transport rate.....		27
25. Comparison of computed versus measured transport rates.....		29

## TABLES

TABLE		Page
1.	Experimental results.....	B7
2.	Computed quantities.....	8
3.	Hydraulic radius, shear stress, and stream power corrected for wall drag by methods of Einstein and of Johnson and Brooks.....	13
4.	Bed-form measurements.....	22

## SYMBOLS

<i>Symbol</i>		<i>Dimensions</i>
<i>a</i>	Coefficient in velocity-shear equation.....	$L^{1/2} T^{-1}$
<i>b</i>	Exponent in velocity-shear equation.....	
<i>c</i>	Bed-form velocity or rate of travel.....	$L T^{-1}$
<i>C</i>	Chezy <i>C</i> .....	$L^{1/2} T^{-1}$
<i>D</i>	Depth of water.....	$L$
<i>f</i>	Darcy-Weisbach <i>f</i> .....	
<i>F</i>	Froude number.....	
<i>g</i>	Acceleration due to gravity.....	$L T^{-2}$
<i>h</i>	Bed-form height.....	$L$
<i>i</i>	Sediment-transport rate.....	$F T^{-1} L^{-1}$
<i>l</i>	Bed-form length (crest to crest).....	$L$
<i>n</i>	Manning <i>n</i> .....	$L^{1/6}$
<i>Q</i>	Water discharge.....	$L^3 T^{-1}$
<i>Q<sub>b</sub></i>	Discharge adjusted to eliminate that part of flow affected by sidewalls.....	$L^3 T^{-1}$
<i>R</i>	Hydraulic radius.....	$L$
<i>R<sub>b</sub></i>	Hydraulic radius of bed (a theoretical hydraulic radius excluding that part of flow cross section which is influenced by sidewalls).....	$L$
<i>S</i>	Slope (ft per ft).....	
<i>t</i>	Temperature (degrees centigrade).....	
<i>V</i>	Mean water velocity.....	$L T^{-1}$
<i>V<sub>s</sub></i>	Surface velocity of water.....	$L T^{-1}$
<i>W</i>	Width of channel.....	$L$
<i>γ</i>	Specific weight of water (=62.4 lbs per cu ft).....	$F L^{-3}$

## SEDIMENT TRANSPORT IN ALLUVIAL CHANNELS

### FLUME EXPERIMENTS ON THE TRANSPORT OF A COARSE SAND

By GARNETT P. WILLIAMS

#### ABSTRACT

A newly constructed 52-foot laboratory flume was used to study sediment transport in a series of 37 runs with a coarse (1.35 mm) sand at water depths of 0.1, 0.3 and 0.5 foot. The data obtained during these runs show that relations between variables can be clarified by maintaining a constant flow depth. For the range of conditions examined, unique relationships were found between any two variables as long as depth was constant. The bed forms ranged from an initial plane bed to antidunes, but ripples and a plane-bed transition from dunes to antidunes did not occur. The data obtained by Gilbert in 1914, using a comparable grain size, agree with the results of the present study. One method of determining the critical flow strength needed to initiate sediment movement indicates that, with the flume and sediment used in this study, the critical flow strength is determined not only by such factors as sediment characteristics and bed slope but also by water depth. (An exception to this last statement was found when shear stress expressed as  $\gamma RS$  was used as the measure of flow strength.) Surface velocity is related to all other variables, particularly to rate of sediment transport.

#### INTRODUCTION

A laboratory flume was constructed in 1964 by the U.S. Geological Survey in Washington, D.C., to explore various problems in sedimentology, geomorphology, and hydrology; its initial use is in the field of sediment transport. Studies of the movement of debris by water aid in the interpretation of numerous geologic processes, pollution, filling of dams and reservoirs, and other phenomena. Use of the laboratory permits the control of many variables which usually cannot be controlled in the natural environment.

Although rivers frequently carry coarse sand and gravel, most previous laboratory studies have dealt with medium and fine sands, with particle diameters less than 1.0 mm. Therefore, coarser grain sand was used in the present sediment-transport experiments. Many of the available data on transport of coarse-grained sand are from the work of G. K. Gilbert (1914) and of E. C. Murphy, who performed most of the experiments in the Gilbert study.

All laboratory investigations require a decision as to which of the pertinent variables should be controlled by the operator. In flume studies, which attempt only to

simulate natural alluvial conditions, the large number of possibly relevant variables can usually be limited to sediment characteristics (such as size, size distribution, shape, density), sediment-transport rate, water discharge, mean velocity, depth, and bed slope and roughness. Other factors, such as water temperature, may have some influence under certain conditions. The sediment characteristics are usually predetermined by the operator and, thus, must be classified as independent variables. In the present study, the sediment-transport rates and the water depths (0.1, 0.3, and 0.5 ft) were also controlled by the operator. The dependent variables, therefore, were water discharge (or mean velocity, at constant depth and width), slope, and bed roughness. (True independence or dependence of variables in sediment transportation is questionable, for the role of each variable in governing other variables or merely reacting to changes in other variables is still poorly understood. Thus, describing a variable as completely dependent or completely independent is both difficult and risky.)

The purposes of this report are to describe the equipment and procedures used in a series of sediment-transport experiments, to present the data of the initial group of a continuing series of experiments, and to examine some of the observed relationships between variables. Certain features of these experiments differ from most previous flume studies on sediment transport, and the data collected during this study will therefore supplement the published information. For example, the use of coarser grained sediment and constant depth in a nonrecirculating flume in this study will provide new data. Although a constant depth is commonly maintained in flume studies in which the water and sediment are continuously recirculated, the writer knows of no studies involving nonrecirculating flumes in which the water depth was held constant.

This investigation was begun under the supervision of Luna B. Leopold, to whom thanks are given for valuable assistance and suggestions throughout the

study—from design and construction of equipment to completion. William W. Emmett assisted in planning the laboratory and performed a major role in the design and construction of the laboratory equipment. Ralph A. Bagnold provided valuable suggestions on various aspects of the investigation. Additional assistance in construction and in some preliminary runs was given by O. Lehn Franke.

## EQUIPMENT AND APPLICATION

### FLUME

The test section of the flume was 52 feet long. The maximum usable width was 4 feet, but for the present experiments an inner trough 1.0 foot wide was used. This trough had transparent plexiglas walls 15 inches high and a wood floor.

At a point 2.0 feet from the downstream end of the flume the plexiglas walls were hinged vertically. Known collectively as the tailgate, these hinged sections could be converged at the end of the flume to dam the water to any desired level. This method was used to make the water depths as uniform as possible.

On top of each of the outer (permanent) flume walls was a rail traversing the entire flume length. On these rails rode a carriage to which was fixed a point gage for depth measurements. The height of the gage tip relative to the rails was read directly from an adjacent scale, to within 0.001 foot.

The slope of the flume was adjustable from horizontal to about 0.02 foot per foot. The test section was hinged at the upstream end. Two large chain hoists, suspended from an independent permanent steel bracing, bore the weight of the flume at the downstream end. The desired slope was obtained by raising or lowering the downstream end of the flume, using these chain hoists.

### WATER CIRCUIT AND DISCHARGE MEASUREMENT

A large sump located below the floor level contained the water supply for the flume. From this sump the water was pumped to a constant-head tank located high on the wall of the building. The water then flowed to the flume by gravity through either or both of two pipes (one 6 in. in diameter, the other 4 in.). The amount of water was regulated by a valve in each pipeline. Excess water was allowed to flow from the constant-head tank directly back to the sump.

Also placed within each line, between the constant-head tank and the flume, was a bend meter for measuring the discharge. This was a common pipe elbow with holes drilled through the wall at the inner and outer vertices of pipe curvature. These holes were connected by tubing to a manometer, and the difference in pressure between the inside and outside parts of the

bend was a direct indication of the discharge flowing through the elbow.<sup>1</sup>

From the constant-head tank, water passed through pipes to a stilling tank (4 ft × 4 ft × 3.4 ft deep) at the head of the flume. From this tank it flowed through a horizontal preliminary channel 1 foot wide and 4 feet long, on the same level as the upstream end of the flume. In passing through this preliminary channel the water was screened by wire mesh to eliminate large-scale disturbances in the flow. The water next went through a 4-foot-long zone where the sediment was fed into the system, and then entered the 52-foot-long flume test section.

As the water-sediment mixture left the flume at the downstream end, it was directed into a collection box. This box had compartments in which the sediment was trapped. The excess water flowed over a lower wall of the box and was channeled back to the sump, thereby completing its circuit.

### SEDIMENT INFEED

Sediment was fed into the stream by gradually raising a supply of sand above the channel level and permitting the flowing water to scour the material off the rising floor and into the test section. The technique used proved to be satisfactory, except for a minor amount of sediment leakage.

The sediment infeed area was a bin 4 feet square and 3.5 feet deep located immediately upstream from the flume test section. Within the bin was a false bottom which could be continuously raised or lowered by means of two screw jacks run by a motor above the bin. Reduction gears between the motor and the screw jacks and a speed control on the motor provided a wide range of rates at which the false bottom could be lifted. The dial setting on the motor-speed control was a direct indication of the rate at which the false bottom was being raised.

Two wooden walls, 4 feet long and 1 foot apart, were fixed onto the false bottom. These were placed in such a position that a straight channel 60 feet long was obtained; the last 52 feet was the flume test section, and the first 8 feet was the preliminary channel and the wooden walls of the infeed section.

Sand was loaded into the 4-square-foot section between the walls of the infeed bin. After the loading, the top of the sand was placed at the same level as the top of the adjacent sand surface in the flume test section. As the area within the wooden walls and the rate at which this area (that is, the false bottom) was being raised were known, it was easy to compute the

<sup>1</sup> Calibration was done at the Hydraulics Laboratory of the Georgia Institute of Technology, and the author gratefully acknowledges that department's kindness in permitting the use of their facilities.

rate at which sediment (immersed weight per unit time) was being exposed to the flow. The dial setting on the motor-speed control was therefore directly related to rate of sediment infeed.

As the false bottom slowly rose, some sand leaked out between the upstream and downstream ends of the false bottom and the walls of the bin. During the course of the investigation this condition proved impossible to correct and served to detract somewhat from an otherwise satisfactory infeed technique. It is believed, nevertheless, that the sand was being introduced into the flume at an approximately constant rate so that the disadvantage was an inability to state exactly what the rate of infeed was at a given dial setting.

#### SEDIMENT-TRANSPORT MEASUREMENT

The water-sediment mixture left the flume and was directed into a partitioned collection box just below the downstream end of the flume. The sediment settled to the bottom of this box, and the excess water flowed over the top of one wall and back into the main circuit. For some of the runs, the water-overflow region of the collecting box was covered with a fine wire screen to insure that no sand escaped from the box. (Little difficulty was encountered, however, because the sand used in the tests was fairly coarse.)

The measured sediment-transport rate represented the total quantity of sand transported, and no distinction could be made between bedload and suspended load. The collection box rested on a large floor scale, and the amount of sand and water in the box was weighed directly at the beginning and end of each run. The gain in sediment (immersed weight) and the time interval between weighings provided the rate of transport. This rate, accordingly, is expressed in pounds (immersed weight) per second per unit channel width. During the actual weighing process, the water-sediment mixture leaving the flume was diverted into a by-pass trough so that the weighing could be done undisturbed.

#### SEDIMENT

The sediment used in the experiments was nearly 100 percent quartz sand of a rather narrow size range (fig. 1). This range was about 0.60–2.50 mm, in terms of sieve aperture, and the median size was 1.35 mm. A visual-accumulation-tube size analysis was also performed, in which the sizes are expressed in terms of fall diameter (that diameter of a quartz sphere having the same fall velocity as a sand grain). The range measured by this method was 0.46–1.25 mm, and the median fall diameter was 0.76 mm. The specific gravity and porosity of the material were 2.66 and 0.445, respectively.

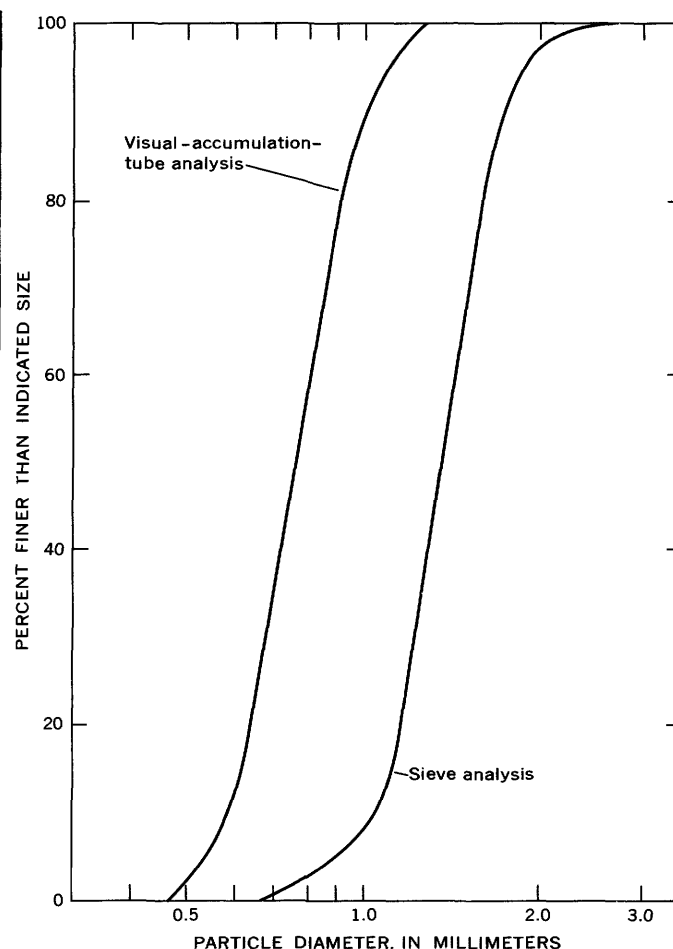


FIGURE 1.—Size analysis of sand.

The fall velocity was determined in a water-filled plastic tube that was 1.35 meters long and had an inner diameter of 29.6 cm. Particles were timed individually over a distance of 100 cm, after allowing 20 cm for the period of acceleration. The average rate of fall for 75 randomly selected grains was 14.5 cm per sec (centimeters per second) at a water temperature of 31.5° C. A correction for temperature (U.S. Inter-Agency Comm. Water Resources, 1957) would adjust this rate to 14.2 cm per sec at 24° C.

#### PROCEDURE

##### INITIATION OF RUNS AND ATTAINMENT OF EQUILIBRIUM CONDITIONS

To begin a run, the operator first decided upon a sediment transport rate and depth (the independent variables). An estimate of the probable discharge and equilibrium slope was then made, and the flume was set at this estimated slope to shorten the time needed to reach equilibrium conditions. Sediment was spread evenly over the floor of the flume to a depth of about 1½–2 inches.



The sediment infeed and discharge were then turned on. By means of several vertical scales at the flume wall a rough estimate of the depth and downstream change (if any) in depth was obtained. If the flow depth was obviously not within an appropriate range (described below), the discharge was altered to change the depth. If, on the other hand, the depth appeared to be within the proper range, no change in discharge was made. The tailgate was adjusted when necessary to raise or lower the water level at the downstream end, until the depth appeared to be uniform throughout the flume.

The next step in the procedure was a rather detailed measurement of depth, slope, and degree of uniformity of depth throughout the flume. This was done by making longitudinal profiles of both the water surface and the bed surface along the center line of the channel. Depth readings were taken with the point gage on each of these surfaces. The horizontal interval at which readings were taken was generally 4 feet, though sometimes 2-foot intervals were used. The readings of depth and distance downstream were plotted on arithmetic scales, and straight lines of best fit were estimated visually for the bed and water surfaces. If these straight-line profiles diverged or converged in a downstream direction, the tailgate opening was changed to make depth uniform. After any change in tailgate setting, additional profile measurements were made, until the lines on the graph indicated a uniform flow.

The perpendicular distance between the two parallel profile lines was taken as the depth of flow. The range of depth tolerance was about  $\pm 7$  percent of the desired depth because experience has shown that errors involved in depth measurements at the higher manageable discharges did not justify attempts at greater accuracy. If necessary, the discharge was adjusted to bring the depth into the range of tolerance; however, it was frequently unnecessary to change the original setting.

Once the desired depth and a uniform flow were established, the slope was allowed to adjust until it became stabilized. Changes in slope were determined by making profile measurements at intervals ranging from 20 minutes to several hours. In many runs no change in slope occurred, indicating that the equilibrium slope was the same as that of the flume itself. In most of the other runs a slight increase in slope, compared to that of the flume, took place.

If the slope changes brought about a decrease or increase in water depth so that depth exceeded the tolerance range, the discharge was adjusted accordingly. Any such alteration in discharge necessitated additional profile measurements, possible tailgate changes, and periods of waiting for any further slope changes, until equilibrium was established.

On a few occasions the slope ceased changing and equilibrium appeared to have been reached; the subsequent profiles, however, indicated that the bed was aggrading or degrading uniformly throughout the flume. Repeat profiles were therefore made in nearly all runs to insure not only that the slope had ceased changing but that the bed and water surfaces were occupying the same spatial elevation with time. The bed elevation (relative to the flume rails) at a given downstream location had to be within  $\pm 3$  percent of the elevation obtained from the previous profile. The criteria for equilibrium, in other words, were (a) constant slope with time and (b) no net gain or loss of sediment in flume, with time. Both of these factors were deduced from the profiles.

If the profiles indicated that the flume was gaining sediment even though the bed slope was not changing, this was interpreted as a need for greater flow strength to accommodate a given sediment infeed. The usual procedure was to open the tailgate. This lowered the water depth downstream and caused scour, so that the overall bed slope was increased. Conversely, if the flume was losing sediment in spite of a constant slope, the tailgate was closed. Usually when this problem occurred, the sediment infeed became depleted before equilibrium conditions could be established, and a new run had to be made. The usefulness of the attempted procedure for arresting bed-elevation changes at constant slope was therefore not conclusively determined.

Most instances of bed-elevation change at constant bed slope occurred in runs at the 0.1-foot depth; in fact, it was difficult to obtain equilibrium conditions at this depth, especially at lesser sediment transport rates. (Rate of sediment supply of course has a direct influence on time required for slope readjustments.) At the 0.1-foot depth, the water-surface profile was particularly sensitive to minor changes of the tailgate and discharge. In a few runs, many days were needed to attain equilibrium at a depth of 0.1 foot. Discharge could generally be adjusted rather early in the experiment, whereas the correct tailgate setting often required considerable time and trial-and-error methods. After some points on the sediment-transport graph had been obtained, the process was somewhat easier, because approximate tailgate settings could be extrapolated before the water was turned on. It was necessary, therefore, to establish a consistent experimental procedure. The writer suspects that the correct tailgate setting can be influenced by the depth to which the sediment is laid down on the flume bottom prior to a run.

Generally, the time needed to reach equilibrium in the experiments varied from about one half hour to many days. (This excludes nights, at which time

the pump was always stopped.) Often a run could be completed in a single day or less. The following factors greatly facilitated the attainment of equilibrium:

1. A high rate of sediment transport (a high value of the fluid flow strength).
2. Depths of 0.3 and 0.5 rather than 0.1 foot.
3. An accurate estimate of the flume slope setting.

Secondary factors which could expedite attainment of equilibrium were an appropriate initial choice of water discharge to provide the desired depth, and good judgment in determining the tailgate opening. By far the greatest hindrance to a prompt attainment of equilibrium was a shallow depth (0.1 ft) or some feature associated with this depth.

### MEASUREMENTS

As soon as equilibrium conditions had been realized, the run was started. This involved a measurement of the following:

1. Discharge, as read from the manometer. This was recorded at the start and finish of each run.
2. Water temperature, also measured at the start and finish of each run.
3. Slope:

(a) The slope of the flume (or more precisely, that of the flume rails upon which the point gage rode) was determined by setting up a surveyor's level independent of the flume structure and measuring the vertical drop in a known distance downstream. The average of two measurements was taken as the final value.

(b) The slope of the bed (and water surface) relative to the flume rails was taken from the plotted profiles. Horizontal profiles on the graph indicated that the bed and water surfaces were parallel to the flume rails. The extent to which the lines departed from the horizontal on the graph reflected the extent to which their inclination departed from that of the flume rails. Slope relative to flume rails and slope of flume rails themselves were combined to give the actual bed (and water surface) slope.

4. Depth, from profiles described in 3b.
5. Sediment-transport rate. An effort was made to collect sediment in the collection box for as long a period as possible. To ensure a representative sediment sample, this period was always long enough to allow at least several (and usually many) bed forms to move out of the flume and into the collection box. This procedure helped obviate possible error due to variations in the transport rate between the trough and the crest of bed forms,

error which was suspected to be the cause of point scatter in sediment-transport diagrams.

### 6. Bed-form characteristics:

(a) General type of bed form and other noteworthy features.

(b) Wavelengths. A rapid traverse was made of the flume length, and in this traverse the location of every well-defined bed-form crest was recorded. From these data an average wavelength could be obtained, as well as an estimate of the degree of uniformity of wavelengths along the flume.

(c) Trough-crest height, perpendicular to bed slope (usually estimated from a scale on the flume wall).

(d) Rate of movement downstream. A single representative bed feature was selected and timed while it passed over a known distance. Occasionally, several bed forms were timed individually and an average rate of movement recorded.

7. Surface velocity. Two or three small pieces of wood were individually timed for rate of movement as they floated along the water surface. (Most pieces were shaved from a stick with a pocket knife and were 1-2 in. long but relatively narrow and flat. In some of the runs at the greater depths, small blocks of woods measuring at most 3 in.  $\times$  1 in.  $\times$  1 in. were used.) The average velocity of the group was taken as the final value. This surface velocity was multiplied by 0.80 to provide a rough estimate of the mean flow velocity, as is explained in the results section. (The actual value of mean velocity was obtained by dividing discharge by cross-sectional area, based on depth as given in profiles.)

8. Sediment samples. Material in the collection box and material left on the bed were sampled after the completion of the run. The samples were dried and then sieved on a Ro-Tap. (The average of 36 such analyses provided the sediment-size characteristics described.)

Photographs were taken, usually during and after the run. Those taken during the run were made from a side view, whereas those taken after the water had drained out of the flume depicted an upstream view.

A pitot static tube was used for velocity measurements in some early runs, but this practice was soon discontinued. Because the bed and water surfaces were often irregular, the vertical height at which the readings were being taken was uncertain. Secondly, any reading was greatly affected by the proximity of a bed form. Finally, the presence of the tube near the bed caused scour in the sediment below the tube, and

the effect of this scoured region on the velocity value could not be determined.

The measured values for several of the variables were checked by various methods. The mean velocity as obtained from the discharge, and depth was compared with the mean velocity as estimated from float measurements. This same estimate of mean velocity could be used with the discharge to provide a check on the depth as obtained from the profiles. Finally, the attainment of equilibrium and the slope value were verified by repeated profile measurements. Repeat readings were taken on many of the variables as a standard procedure.

Runs in which mean flow velocities were greater than about 3.5 ft per sec could not be made with the present equipment. Faster velocities could not be investigated because the supply of sediment in the submerged infeed bin was depleted before all of the necessary experimental measurements could be completed. Also, at the 0.5-foot depth the maximum water capacity of the flume system was nearly reached.

No convenient method was available for maintaining a constant water temperature. In most runs the water temperature ranged from 11° to 27°C. Temperature during any run varied only a degree or two, if at all. A significant temperature effect on rate of sediment transport is doubtful for the grain sizes used in this study. According to Colby and Scott (1965), the percentage change in bed-material discharge that accompanies a particular temperature change is generally small for particles 1 mm in diameter or larger.

Reproducibility at depths of 0.3 and 0.5 foot was excellent. Attempts were not made to reproduce any of the runs at the 0.1-foot depth.

Run 23 was conducted with the flume horizontal rather than at a slope. This procedural deviation was made because colleagues suggested that the setting of the flume at some particular slope (prior to the run) was prejudicing the final slope value. That is, they felt that a range of equilibrium slopes was possible; the measured slope value might be a minimum possible slope, a maximum possible slope, or some intermediate slope, depending on how the operator performed the experiments. For a given depth and velocity, the various possible values of slope could presumably be accommodated by changes in the bed roughness. Run 23 satisfied the stated prerequisites for equilibrium and is therefore included in the results, but no insight was obtained into a possible range of slope values. The physical conditions within the flume during run 23 unavoidably differed in one respect from the conditions of all other runs. The entrance region in the flume was positioned vertically in such a way that after the sand wedge had formed in the flume, the water passing

through the infeed section had to flow very slightly uphill before coursing over the sand in the flume. This difference in conditions was sufficient to cause diagrams for run 23 to be distinguishable from diagrams for other runs made at a similar depth in many of the illustrations presented later in this report. The horizontal flume showed the following disadvantages:

1. The total time needed to conduct a run increased about tenfold. Some of the extra time was required for slope adjustments by the water-sediment mixture, and some was required for temporarily stopping the run to refill the sediment-infeed bin.
2. The maximum discharge capacity of the flume was drastically reduced by the large amount of sand that accumulated in the flume.
3. About 1½-2 times as much sediment was needed to perform a run, because so much sediment was stored in the wedge within the flume.

## RESULTS

### GENERAL

The measured and computed values for all runs, excluding bed-form data, are listed in tables 1 and 2. In these tables the runs made at each of the three depths have been arranged in order of increasing sediment-transport rate. The bed configurations ranged from plane bed to antidunes. A plane-bed stage between dunes and antidunes did not occur. (Bed forms are discussed later.) Sediment movement was always in the form of bedload, according to visual observation, and little if any material was transported as suspended load. The size distribution of material caught in the collection box did not differ significantly from that of material remaining on the flume bed.

### SEDIMENT-TRANSPORT RATES

Various measures of the strength of flowing water can be related to the rate at which sediment is transported. Examples of such measures are the following:

1. Stream power. The power for a whole channel can be defined as the product of the weight of fluid (in pounds) flowing per second and the energy per unit weight of fluid (in foot pounds per pound). This product can be written as  $\gamma Q \times \text{energy}$ , where  $\gamma$  = specific (unit) weight of water and  $Q$  = discharge of water. The dimensions are  $FLT^{-1}$ . When the flow is uniform the energy loss per foot of channel length is given by the slope  $S$ , so that the power per unit length of channel becomes  $\gamma QS$  (dimensions  $FT^{-1}$ ). The stream power per unit bed area is then  $\gamma QS/W$ , where  $W$  = channel width. The dimensions are  $FL^{-1}T^{-1}$ , pounds per second

TABLE 1.—*Experimental results*

Run	Q (cfs)	S (ft per ft)	D (ft)	V (fps)	Sediment transport		R (ft)	t (°C)	V <sub>c</sub> (fps)
					Measurement period (sec)	i (lbs per sec per ft)			
1	0.127	0.00411	0.100	1.27	17,940	0.00145	0.083	18.5	1.68
2	.142	.00495	.100	1.41	10,140	.00291	.083	19.2	1.89
3	.158	.00590	.102	1.55	5,400	.00593	.085	21.0	2.08
4	.154	.00751	.101	1.53	2,460	.00935	.084	12.5	2.22
5	.166	.01082	.095	1.75	1,440	.01980	.080	11.9	2.41
6	.191	.01280	.101	1.89	1,684	.03444	.084	17.6	2.67
7	.220	.01505	.099	2.22	2,183	.05772	.083	15.5	2.86
8	.233	.01992	.094	2.48	960	.11200	.079	23.5	3.39
9	.292	.02218	.097	3.01	473	.16810	.081	24.7	3.85
10	.405	.00110	.297	1.36	24,180	.00025	.186	21.3	1.56
11	.440	.00121	.314	1.40	26,040	.00031	.193	22.7	1.67
12	.440	.00136	.313	1.41	23,820	.00054	.193	19.8	1.76
13	.438	.00162	.294	1.49	23,400	.00107	.185	18.6	1.85
14	.452	.00182	.294	1.54	12,240	.00171	.185	16.5	1.87
15	.470	.00200	.300	1.57	14,040	.00256	.188	18.4	2.06
16	.498	.00210	.303	1.64	6,360	.00361	.189	17.2	2.16
17	.503	.00211	.304	1.65	2,400	.00375	.189	17.8	2.10
18	.512	.00236	.295	1.74	5,040	.00585	.186	17.1	2.14
19	.530	.00272	.294	1.80	3,620	.00925	.185	17.8	2.30
20	.551	.00318	.290	1.90	2,340	.01090	.183	16.1	2.31
21	.570	.00397	.288	1.98	2,160	.01597	.183	16.2	2.50
22	.650	.00509	.287	2.26	1,980	.03156	.182	15.9	2.92
23	.790	.00471	.298	2.65	2,940	.03262	.187	30.8	2.86
24	.741	.00557	.297	2.49	2,130	.03826	.186	12.3	2.92
25	.794	.00643	.306	2.59	1,353	.04805	.190	15.5	3.05
26	.860	.00721	.307	2.80	960	.06875	.190	21.8	3.33
27	1.050	.00824	.324	3.24	720	.09722	.197	23.5	3.67
28	1.120	.01088	.321	3.49	510	.16280	.194	25.0	3.74
29	.845	.00137	.509	1.66	14,040	.00203	.252	21.0	1.91
30	.795	.00133	.485	1.64	9,180	.00207	.246	26.0	1.92
31	.866	.00144	.505	1.72	10,020	.00288	.251	22.9	1.97
32	.905	.00172	.517	1.75	8,460	.00479	.254	23.6	2.02
33	.960	.00184	.512	1.87	18,420	.00610	.253	23.2	2.25
34	.958	.00216	.502	1.91	3,840	.00716	.250	17.9	2.20
35	1.050	.00251	.517	2.03	6,300	.01128	.254	18.7	2.38
36	1.100	.00314	.504	2.18	2,640	.01970	.250	20.8	2.54
37	1.320	.00416	.510	2.59	1,800	.03333	.252	20.8	3.14

per foot; these same units are used to measure the sediment-transport rate.

2. Shear stress based on depth. The shear, or tractive force, exerted on a unit bed area is commonly defined as the weight of the water above the unit bed area times the slope of the channel. The volume of water (area $\times$ depth) above a unit bed area will be numerically equal to the depth of the water  $D$ , and the weight will therefore be given by  $\gamma D$  (dimensions  $FL^{-2}$ ). The shear per unit bed area is therefore  $\gamma DS$ , in pounds per square foot.
3. Shear stress based on hydraulic radius. For very wide channels the depth is equal to the hydraulic radius  $R$ , so that the shear stress over a unit bed area would be  $\gamma RS$ . The shear stress computed in this manner is assumed to represent an average shear per unit area of channel boundary. However, for narrow sediment-bearing channels with smooth sidewalls the shear probably is not

equally distributed over the walls and floor of the channel; the computed shear stress is then of questionable value.

4. Mean water velocity  $V$ , defined as  $Q/WD$ .
5. Regime theory bed factor,  $V^2/D$ . (Except for a gravitational constant  $g$ , this is the square of the Froude number  $F$ , where  $F=V/\sqrt{gD}$ .)

No single measure of flow strength has yet gained widespread acceptance. A meaningful comparison might be obtained by relating the sediment-transport rate ( $i$ ) to each of the measures listed above. The relations are shown in figures 2–6.

Several features are immediately noticeable in these diagrams. First, if depth is held constant, in any plot the data for any chosen depth fall on a single curve and show very little point scatter. This fact should be emphasized because it suggests that permitting the depth to vary may well cause much of the scatter found in sediment-transport diagrams. (Although it

TABLE 2.—Computed quantities

Run	$QS (\times 10^3)$	$RS (\times 10^3)$	$DS (\times 10^3)$	$V^2/D$	$W/D$	$V/V_c$	Chezy $C$	Darcy-Weisbach $f$	Manning $n$	Froude No. $F$
1-----	0.522	0.342	0.411	16.1	10.00	0.76	68.7	0.0546	0.0142	0.71
2-----	.703	.412	.495	19.9	10.00	.75	69.5	.0533	.0141	.79
3-----	.932	.500	.602	23.6	9.80	.75	69.2	.0537	.0142	.86
4-----	1.16	.631	.758	23.2	9.90	.69	61.0	.0692	.0161	.85
5-----	1.80	.863	1.03	32.2	10.52	.73	59.5	.0727	.0163	1.00
6-----	2.44	1.075	1.29	35.4	9.90	.71	57.6	.0775	.0170	1.05
7-----	3.31	1.243	1.49	49.8	10.10	.78	63.1	.0647	.0155	1.25
8-----	4.64	1.576	1.87	65.4	10.63	.73	62.5	.0660	.0155	1.43
9-----	6.48	1.800	2.15	93.4	10.30	.78	71.0	.0511	.0137	1.70
10-----	.445	.205	.327	6.2	3.36	.87	95.1	.0284	.0117	.44
11-----	.532	.233	.380	6.2	3.18	.84	91.5	.0307	.0125	.44
12-----	.598	.262	.426	6.4	3.19	.80	87.0	.0339	.0125	.44
13-----	.710	.300	.476	7.6	3.40	.81	86.1	.0347	.0130	.48
14-----	.823	.337	.535	8.1	3.40	.82	83.7	.0367	.0135	.50
15-----	.940	.375	.600	8.2	3.33	.76	80.9	.0393	.0138	.51
16-----	1.05	.396	.636	8.9	3.30	.76	84.5	.0360	.0135	.53
17-----	1.06	.398	.641	9.0	3.28	.79	82.9	.0374	.0135	.53
18-----	1.21	.438	.696	10.3	3.38	.81	83.3	.0371	.0134	.56
19-----	1.44	.504	.800	11.0	3.40	.78	80.4	.0398	.0139	.59
20-----	1.75	.584	.922	12.4	3.44	.82	78.5	.0417	.0142	.62
21-----	2.26	.725	1.14	13.6	3.47	.79	73.6	.0475	.0152	.65
22-----	3.31	.928	1.46	17.8	3.48	.77	74.1	.0469	.0151	.74
23-----	3.72	.880	1.40	23.6	3.36	.93	89.2	.0323	.0125	.86
24-----	4.13	1.038	1.65	20.9	3.36	.85	77.3	.0430	.0145	.81
25-----	5.10	1.220	1.97	21.9	3.26	.85	74.2	.0467	.0151	.83
26-----	6.20	1.371	2.21	25.5	3.25	.84	75.7	.0449	.0148	.89
27-----	8.65	1.620	2.67	32.4	3.08	.88	80.6	.0396	.0140	1.00
28-----	12.19	2.100	3.49	37.9	3.11	.93	76.2	.0443	.0148	1.09
29-----	1.16	.346	.697	5.4	1.96	.87	89.3	.0323	.0132	.41
30-----	1.06	.327	.645	5.5	2.06	.85	90.6	.0313	.0129	.42
31-----	1.25	.362	.727	5.9	1.98	.87	90.5	.0314	.0130	.43
32-----	1.56	.437	.889	5.9	1.94	.87	83.7	.0367	.0141	.43
33-----	1.77	.465	.942	6.8	1.95	.83	86.6	.0343	.0136	.46
34-----	2.07	.541	1.084	7.3	1.99	.87	82.3	.0379	.0143	.47
35-----	2.64	.638	1.30	8.0	1.94	.85	80.2	.0400	.0147	.50
36-----	3.45	.788	1.58	9.4	1.98	.86	77.9	.0424	.0151	.54
37-----	5.49	1.050	2.12	13.2	1.96	.82	79.9	.0403	.0147	.64

may be possible by interpolation to sketch lines of constant depth for data from runs in which depth was allowed to vary, such a procedure would certainly be much less precise.) Thus, although the general depth effect could be perceived regardless of how the experiments were run (depth constant from run to run or depth varying), the maintenance of a constant depth permitted more accurate determination of the relations.

A second characteristic of the graphs is that, with the exception of the  $\gamma RS$  plot, a unique relationship does not exist between the measures of flow strength and sediment-transport rate. A given rate of sediment movement, as the independent or imposed variable, can be accommodated by various values of  $\gamma QS$ ,  $V$ ,  $\gamma DS$ , and  $V^2/D$ . Conversely, according to figures 2, 3, 5, and 6, a given flow strength can transport sediment at various rates. The determining factor on these diagrams is the water depth. Surprisingly, if shear expressed as  $\gamma RS$  is used as the measure of flow strength, the effect of depth is practically eliminated, and all the data can be described by a single curve (fig. 4). On the other four diagrams, however, the depth effect is

evident, though to differing extents. The velocity-transport relation suggests that the effect of depth might be eliminated at slightly greater depths on this particular plot. There may be a tendency on the  $V^2/D$  graph for the lines of greater depths to converge, but this plot has magnified the depth effect more than any of the others. Such an influence may or may not be desirable. The diagrams of stream power and shear ( $\gamma DS$ ) do not seem to show any tendency to eliminate the influence of depth for the range of conditions examined. Power and shear ( $\gamma DS$ ) both involve a depth-slope product, so that in a laboratory flume the main distinction between the two is the inclusion of mean velocity in the computation of stream power. Significantly, the same depth-slope product (or velocity-depth-slope product) can give different sediment-transport rates. As depth increases, with a corresponding reduction of slope so that  $DS$  remains constant, the sediment-transport rate decreases. The general depth effect on sediment-transport rates was discussed by Colby (1964b, p. A25-A29).

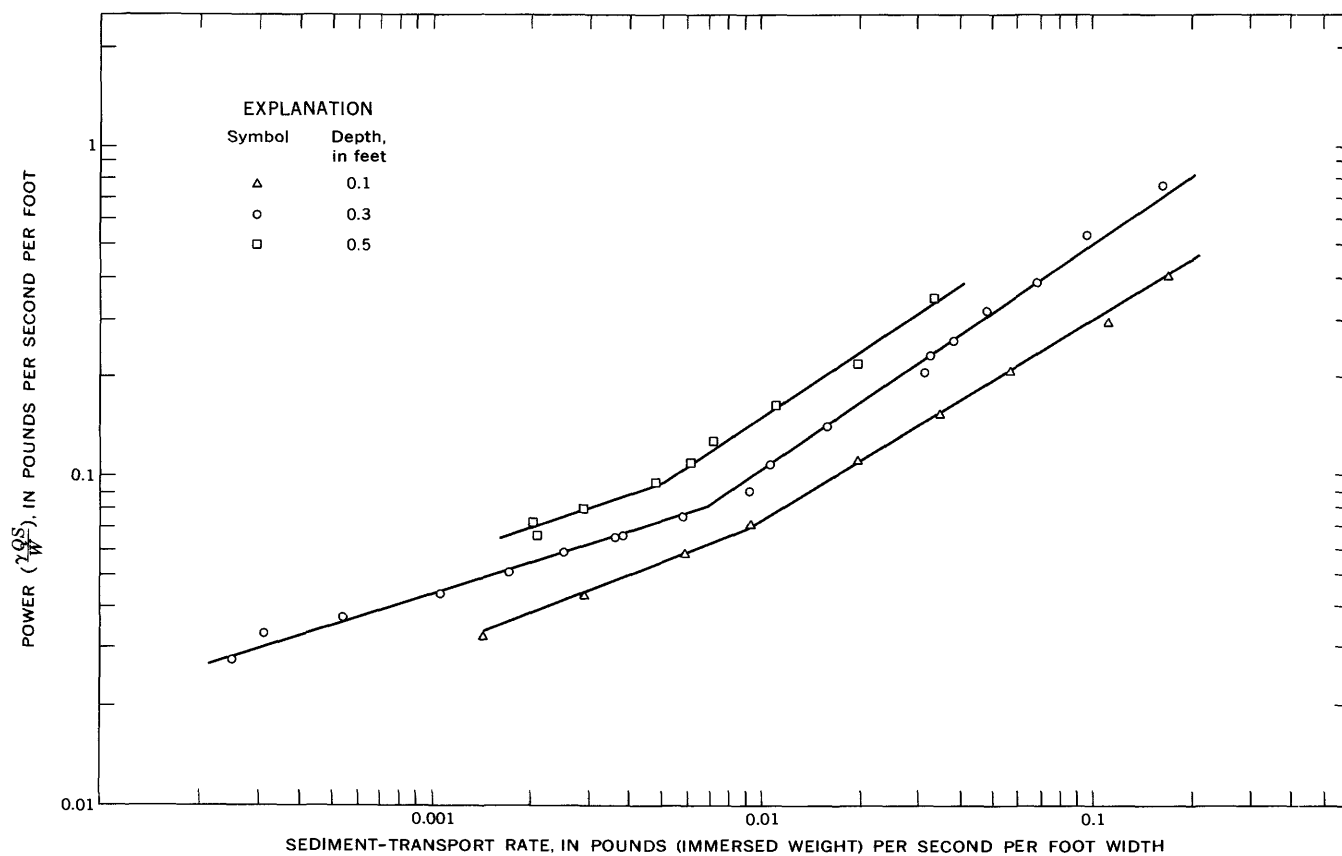
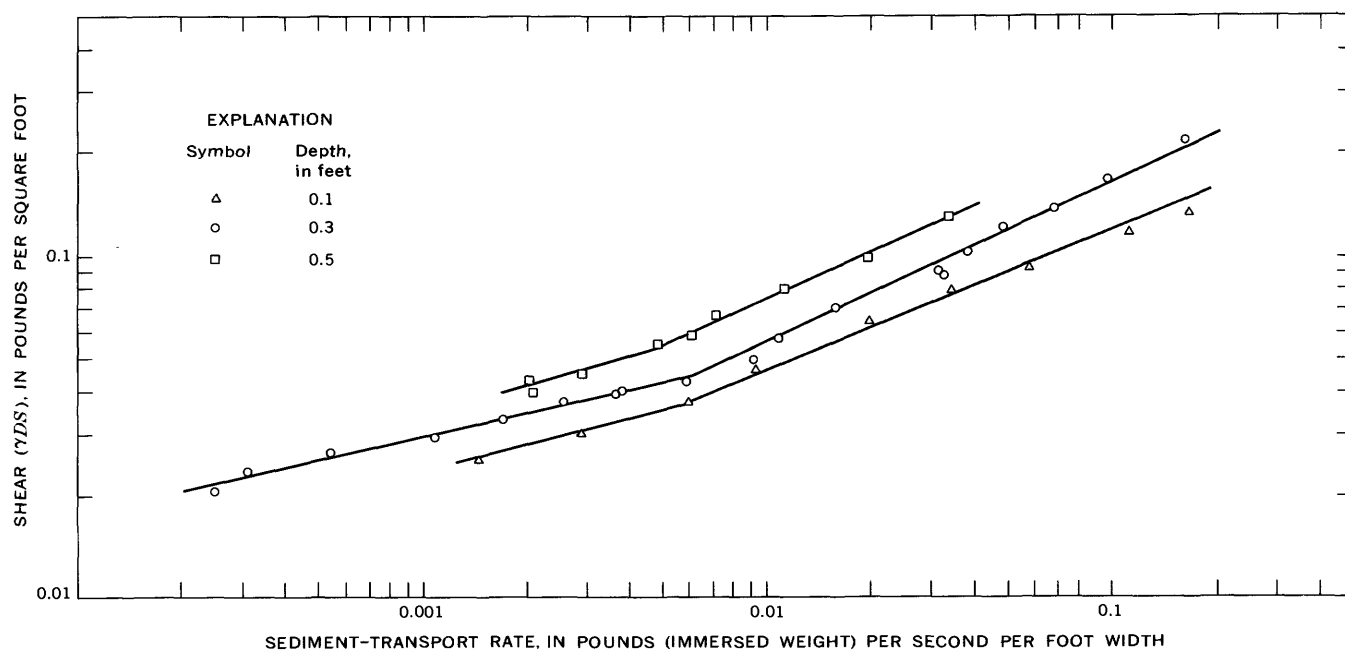


FIGURE 2.—Power versus transport relation.

FIGURE 3.—Shear ( $\gamma DS$ ) versus transport relation.

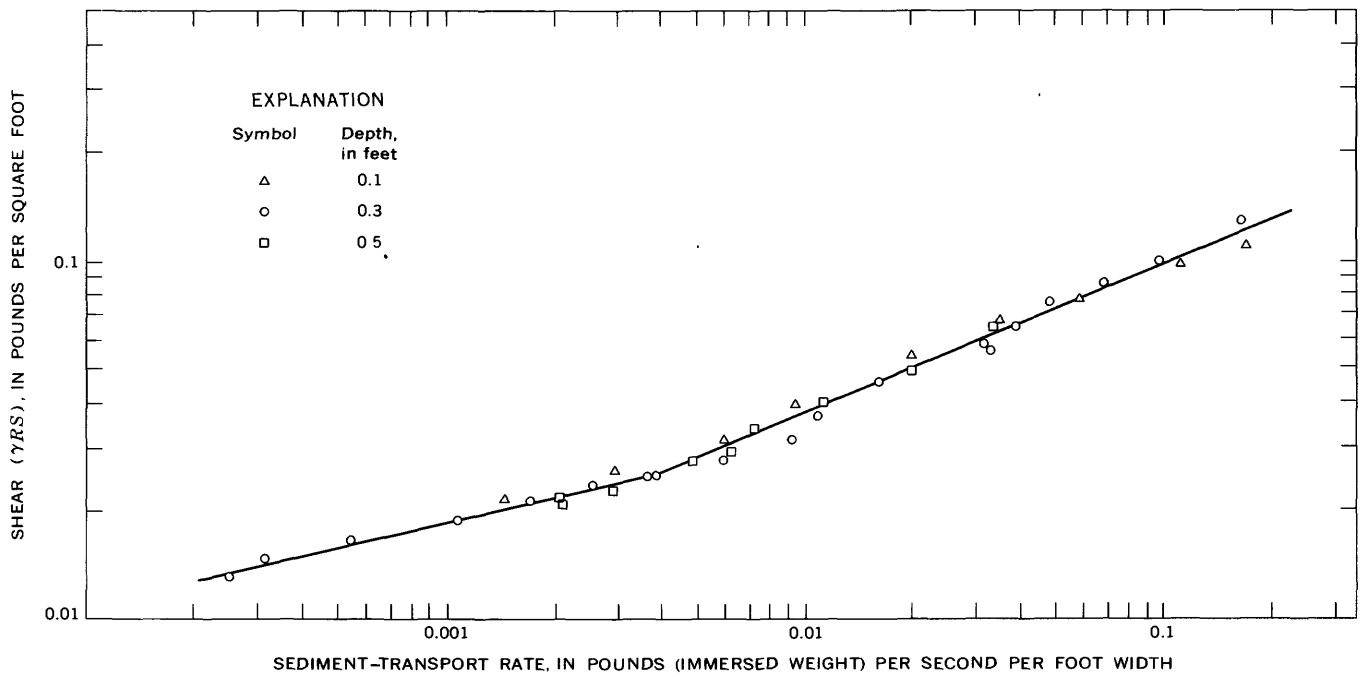
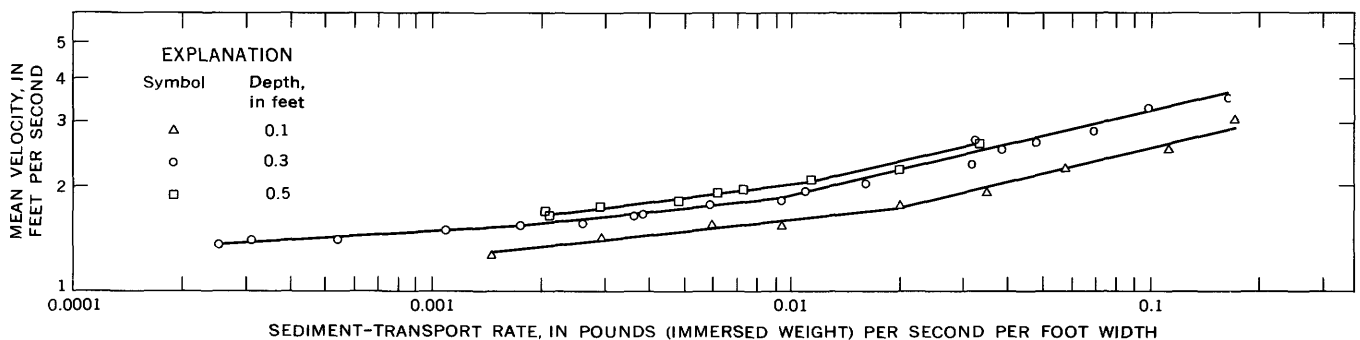
FIGURE 4.—Shear ( $\gamma RS$ ) versus transport relation.

FIGURE 5.—Mean velocity versus transport relation.

The fact that a given flow strength, as defined by  $\gamma QS$ ,  $V$ ,  $\gamma DS$ , and  $V^2/D$ , can be related to various sediment-transport rates may be a reason for some of the difficulties encountered in seeking reliable sediment-transport formulas.

What determines the particular  $DS$  or  $QS$  combination that will be derived for a given sediment load? When sediment suddenly enters a reach of stream at a faster rate, does the slope remain constant and the depth increase to provide the necessary flow strength? A current hypothesis (Langbein, 1964) asserts that each dependent variable will change in value by equal and least possible increments, insofar as permitted by limitations within the system.

A single straight line cannot be fitted to the plot of data for the present runs at a given depth, regardless of which measure of flow strength is involved. All the relations exhibit a change in the trend of the data

plot near  $0.004 < i < 0.01$  lb per sec per ft. A straight line fits the points below this range, and a steeper straight line fits the data above this range. If the zone where the trend changes is regarded as a boundary between a low transport range and a higher transport range, the relations shown in figures 2-6 are approximately as follows:

*Low transport range*

$$\gamma QS \propto i^{0.37}$$

$$\gamma DS \propto i^{0.24}$$

$$\gamma RS \propto i^{0.23}$$

$$V \propto i^{0.09}$$

$$V^2/D \propto i^{0.17}$$

*Higher transport range*

$$\gamma QS \propto i^{0.65}$$

$$\gamma DS \propto i^{0.46}$$

$$\gamma RS \propto i^{0.42}$$

$$V \propto i^{0.25}$$

$$V^2/D \propto i^{0.48}$$

All the relations show the change in trend, so there is little probability that this particular feature is due to any selected measure of flow strength. Rather, it would seem that within the indicated zone some physical change actually occurs in the mechanics of

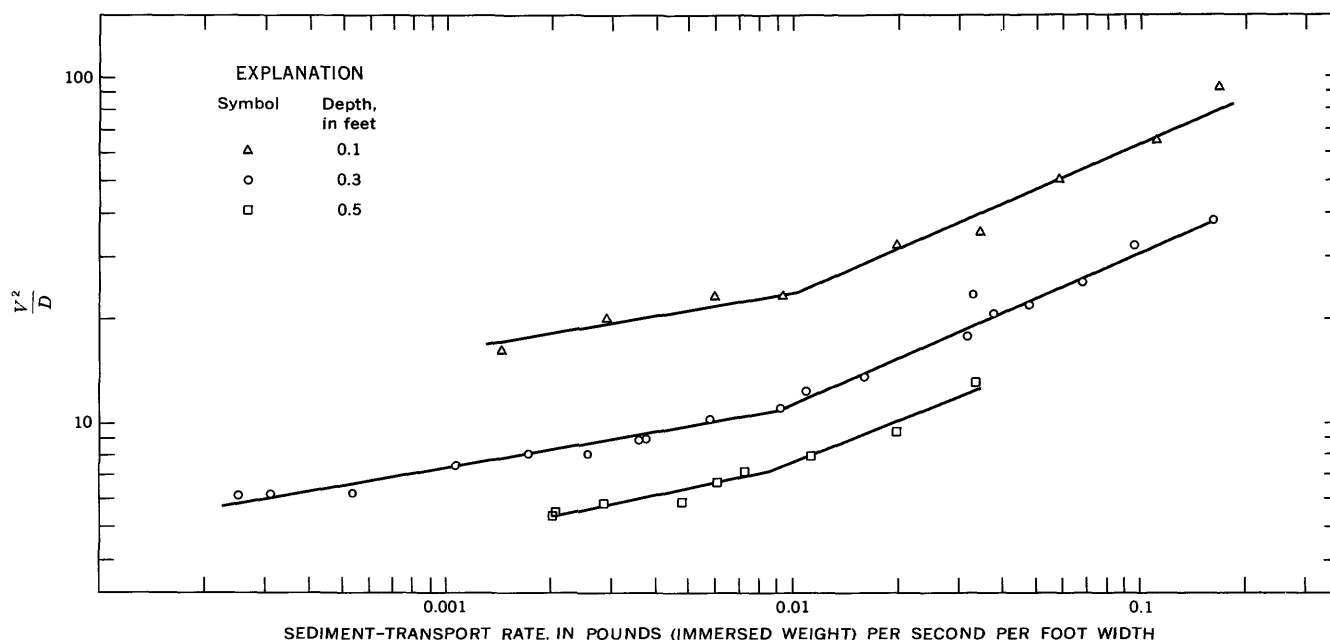


FIGURE 6.—Regime bed factor versus transport relation.

the water-sediment relationship. The present data do not explain this phenomenon.

The steepness of the fitted lines indicates that, for the conditions examined in this study, the measure of flow strength which seems to be most sensitive to changes in sediment-transport rate is the mean velocity. A small change in  $V$  is associated with a large change in  $i$ . The least sensitive measure appears to be stream power. A 10-percent error in stream power, in other words, would provide a more accurate estimate of a given sediment-transport rate than would a 10-percent error in mean velocity. This is true whether or not the water depth is known. An evaluation of power, however, involves the measurement of an additional variable (slope); thus, there is a greater likelihood of error in the power value. Colby (1964a; 1964b) compared several of the currently popular measures of flow strength in connection with sediment transport.

Critical, or threshold, flow strength is the minimum flow strength that will transport sediment. Two methods are known to the writer for determining this value. One method is by visual means and is very subjective; owing to irregularity of particle movements, this approach is generally considered difficult. The second method is to extrapolate a sediment-transport curve down to zero or near-zero values of sediment transport and to accept the indicated value of flow strength. For the present purpose, suppose that the accepted lowest rate of continuous sediment transport is 0.0001 lbs per sec per ft. (Visual observations during the actual runs suggest that this is a reasonable

figure.) Extrapolating the stream-power lines (fig. 2) down to this transport rate shows the critical power to be about 0.0122, 0.0215, and 0.0245 lb per sec per ft at depths of 0.1, 0.3, and 0.5 foot, respectively. The same procedure can be applied to the plots of shear expressed as  $\gamma DS$ , mean velocity, and the bed factor (figs. 3, 5, 6). The inescapable conclusion is that, at least for the grain size used in this flume, unique values for such factors as critical power and critical shear ( $\gamma DS$ ) do not exist. Instead, a different value of critical flow strength is obtained for each depth examined. However, if  $\gamma RS$  is used as the measure of flow strength (fig. 4), only one value of threshold shear exists, regardless of depth.

Because the same flow strength (except the  $\gamma RS$  data) moves different quantities of sediment at different depths, it is likely that any expression of the critical flow strength (except  $\gamma RS$ ) will have to refer to a specific water depth, at least for channels and sediment similar to those studied here. This depth influence has been considered only in some proposed definitions of critical flow strength. (See Sundborg, 1956, p. 177.) For the present data (unless  $\gamma RS$  is used as the measure of flow strength), any definition of threshold flow strength that is based only on sediment characteristics, and perhaps on bed slope, and which is not adjusted to resolve the depth effect, would appear to be inadequate. Such expressions may be in error in proportion to a certain range of water depths. According to this investigation, such a depth range generally extends from 0.1 to 0.5 foot, and the range is probably somewhat



greater than this. Note that the problem is not necessarily solved by including depth in the computation of the flow strength ( $\gamma DS$ ). The present data imply that, for comparable sedimentary material, the only possibility of avoiding the determination of a different critical flow strength for each depth in a channel 1 foot wide lies in the use of  $\gamma RS$  as the measure of flow strength, or in the hope that depth suddenly ceases to play a major role in sediment transport at extremely low transport rates. The latter possibility seems remote, according to the curves in figures 2, 3, 5, and 6.

Why are the data in most of the plots segregated on the basis of depth? This question would seem to warrant some attention in future laboratory research. One possible influence, suggested by Einstein and by Bagnold in written communications (1965) is the drag exerted by the smooth sidewalls. A greater depth means that a greater sidewall area is in contact with the moving fluid, so that the wall drag increases as depth increases. Thus for given values of stream power, mean velocity, and such factors, the additional wall drag associated with a greater depth would result in a greater overall retardation of the movement of water and of sediment. In other words, for a given flow strength, a greater depth would mean a lesser rate of sediment transport. If wall drag is the sole cause of the segregation of points, then presumably if the same 37 runs were conducted in a much wider channel, all the plotted points would fall on a single line regardless of flow depth. (On the other hand, the question then arises as to how such data would plot if  $\gamma RS$  is used as the measure of flow strength.) Another possible cause of the segregation, suggested by Bagnold, is the height to which the saltating grains rise into the body of the flow; that is, the ratio of saltation height to flow depth. The transport rate might be expected to be greater at shallow flow depths because the saltation zone occupies a larger proportion of the whole flow depth. As Bagnold (written commun., 1965) pointed out, if this is true, the variation with depth is a small-scale phenomenon only, and would disappear progressively as depth is increased (provided of course that any wall-drag effect in narrow channels is also taken into account). Another proposal (Colby, 1964b) focuses attention on the vertical distribution of velocity. In comparing a shallow depth and a deeper one, the same value of mean velocity for both depths would require that the velocity increase much faster with height above the bed for the shallower depth. Consequently, the given mean velocity would occur much closer to the sand bed in the shallower depth. In other words, velocities at a given distance from the bed (in the lower part of the full depth, at least) would be greater in runs at the

shallower depth, and, hence, more sediment would be moved.

The sidewalls of the flume undeniably exert some drag on the flow, and curiosity naturally arises as to whether the same values of flow strength would be required to move sediment at the present transport rates in a channel of "infinite" width—that is, a channel wide enough that any sidewall influence is negligible. Two theoretical proposals for adjusting data obtained in narrow channels to eliminate the wall-drag effect are the method of Einstein (1942) and the method of Johnson as modified by Brooks (1954)—herein called the Einstein and the Johnson-Brooks methods. Briefly, these methods divide the flow cross section into that part influenced by sidewalls and that part in the center of the channel, unaffected by sidewalls. A hydraulic radius  $R_b$  is calculated for the latter part. A bed shear stress  $\gamma R_b S$  can then be computed which presumably represents the shear acting on the bed and omits that part of the shear acting on the sidewalls. Furthermore, because the hydraulic radius  $R$  for an infinitely wide channel is equal to  $R_b$  (wall drag negligible) and is also equal to the mean depth, the computed  $R_b$  is equal to a depth  $D_b$  which would be obtained if that part of flow affected by sidewalls were removed. If mean velocity and bed width are considered to be unchanged, a new discharge  $Q_b$  can therefore be computed, where  $Q_b = VD_b W$  or  $Q_b = VR_b W$ . This would be the discharge if the velocity and bed width were to remain but flow affected by sidewalls were excluded. Such a discharge can presumably be used in sediment-transport relations to represent the discharge free of wall drag. Thus, stream power unaffected by sidewalls would be  $\gamma Q_b S / W$ . The main distinction between the two methods is that Einstein's is based on the Manning formula, whereas the Johnson-Brooks approach uses the Darcy-Weisbach relation. Both methods have been applied to the present data, and the computed values are listed in table 3.

It can be noted from table 3 that at  $D=0.1$  foot the two methods produce almost the same values of  $R_b$ . At the other two depths the Johnson-Brooks procedure yields values which are about 3–6 percent greater than the values obtained by the Einstein method, and differences of this magnitude are considered rather slight. For both methods the calculations are not difficult and require about the same amount of time. The adjusted values of flow strength obtained using the Einstein method are plotted against sediment-transport rate in figure 7. (The constant  $\gamma$  has not been included in the computations of flow strength.) In regard to the power-transport relations, the lines for the various depths are slightly closer together compared with the  $\gamma QS/i$  diagram of figure 2. There still exists, however,

TABLE 3.—Hydraulic radius, shear stress, and stream power corrected for wall drag by methods of Einstein and of Johnson and Brooks

Run	Einstein			Johnson-Brooks		
	$R_b$ (ft)	$R_b S$ ( $\times 10^3$ )	$Q_b S = VR_b S$ ( $\times 10^3$ )	$R_b$ (ft)	$R_b S$ ( $\times 10^3$ )	$Q_b S = VR_b S$ ( $\times 10^3$ )
1.....	0.091	0.374	0.475	0.092	0.378	0.481
2.....	.091	.450	.635	.092	.455	.642
3.....	.092	.543	.842	.094	.555	.860
4.....	.093	.698	1.068	.095	.713	1.091
5.....	.088	.952	1.666	.090	.974	1.705
6.....	.094	1.203	2.274	.095	1.216	2.298
7.....	.091	1.370	3.041	.093	1.400	3.108
8.....	.087	1.733	4.298	.089	1.773	4.397
9.....	.088	1.952	5.876	.090	1.996	6.008
10.....	.215	.237	.322	.221	.243	.330
11.....	.230	.278	.389	.238	.288	.403
12.....	.235	.320	.451	.244	.332	.468
13.....	.224	.363	.541	.232	.376	.560
14.....	.227	.413	.636	.235	.428	.659
15.....	.229	.458	.719	.243	.486	.763
16.....	.234	.491	.805	.241	.506	.830
17.....	.235	.496	.818	.243	.513	.846
18.....	.228	.538	.936	.238	.562	.978
19.....	.231	.628	1.130	.241	.656	1.181
20.....	.230	.731	1.389	.239	.760	1.444
21.....	.235	.933	1.847	.244	.969	1.919
22.....	.233	1.186	2.680	.243	1.237	2.796
23.....	.223	1.050	2.783	.237	1.116	2.957
24.....	.237	1.320	3.287	.248	1.381	3.439
25.....	.247	1.588	4.113	.259	1.665	4.312
26.....	.246	1.774	4.967	.258	1.860	5.208
27.....	.251	2.068	6.700	.268	2.208	7.154
28.....	.255	2.774	9.681	.269	2.927	10.215
29.....	.348	.477	.792	.363	.497	.825
30.....	.331	.440	.722	.346	.460	.754
31.....	.342	.492	.846	.359	.517	.889
32.....	.368	.633	1.108	.385	.662	1.159
33.....	.357	.657	1.229	.377	.694	1.298
34.....	.363	.784	1.497	.381	.823	1.572
35.....	.376	.944	1.916	.398	.999	2.028
36.....	.375	1.178	2.568	.394	1.237	2.697
37.....	.373	1.552	4.020	.397	1.652	4.279

a definite segregation of fitted lines on the basis of depth. For the shear ( $\gamma RS$ ) versus transport relation it will be recalled that the unadjusted data could be described by a single line (fig. 4). The adjusted shear values show no prominent depth segregation at low transport rates, where the slope of the fitted line is small. As  $i$  increases, a slight depth influence becomes noticeable; and in this higher transport range, it appears that a separate line should be assigned to each water depth. A depth segregation would be slightly more pronounced if the Johnson-Brooks figures were used.

In general, the application of the two methods for eliminating the wall-drag influence tends to support the observation that, for a given value of flow strength, the transport rate increases as depth decreases, for the present sediment and flow conditions. A shear ( $\gamma RS$ ) versus transport diagram may show a depth segregation for wide channels, according to figure 7.

#### RELATIONS OF VARIABLES

The relation of mean velocity to the independent variables transport rate and depth is shown in figure 5. From the given sediment-transport rate and the depth, velocity was uniquely determined.

Discharge was also uniquely determined by sediment-transport rate and depth (fig. 8). The slope of the fitted line for any depth was not constant for the whole range of conditions studied. At low sediment-transport rates  $Q$  varied as  $i^{0.10}$ . But the slopes seemed to undergo a change near  $i \approx 0.01$  lb per sec per ft, becoming slightly steeper ( $Q \propto i^{0.25}$ ) for transport rates somewhat greater than this. The break in the relation appeared to occur at lesser values of  $i$  as depth was increased.

Slope was also uniquely related to transport rate and depth, as can be seen in figure 9. The plot again

## SEDIMENT TRANSPORT IN ALLUVIAL CHANNELS

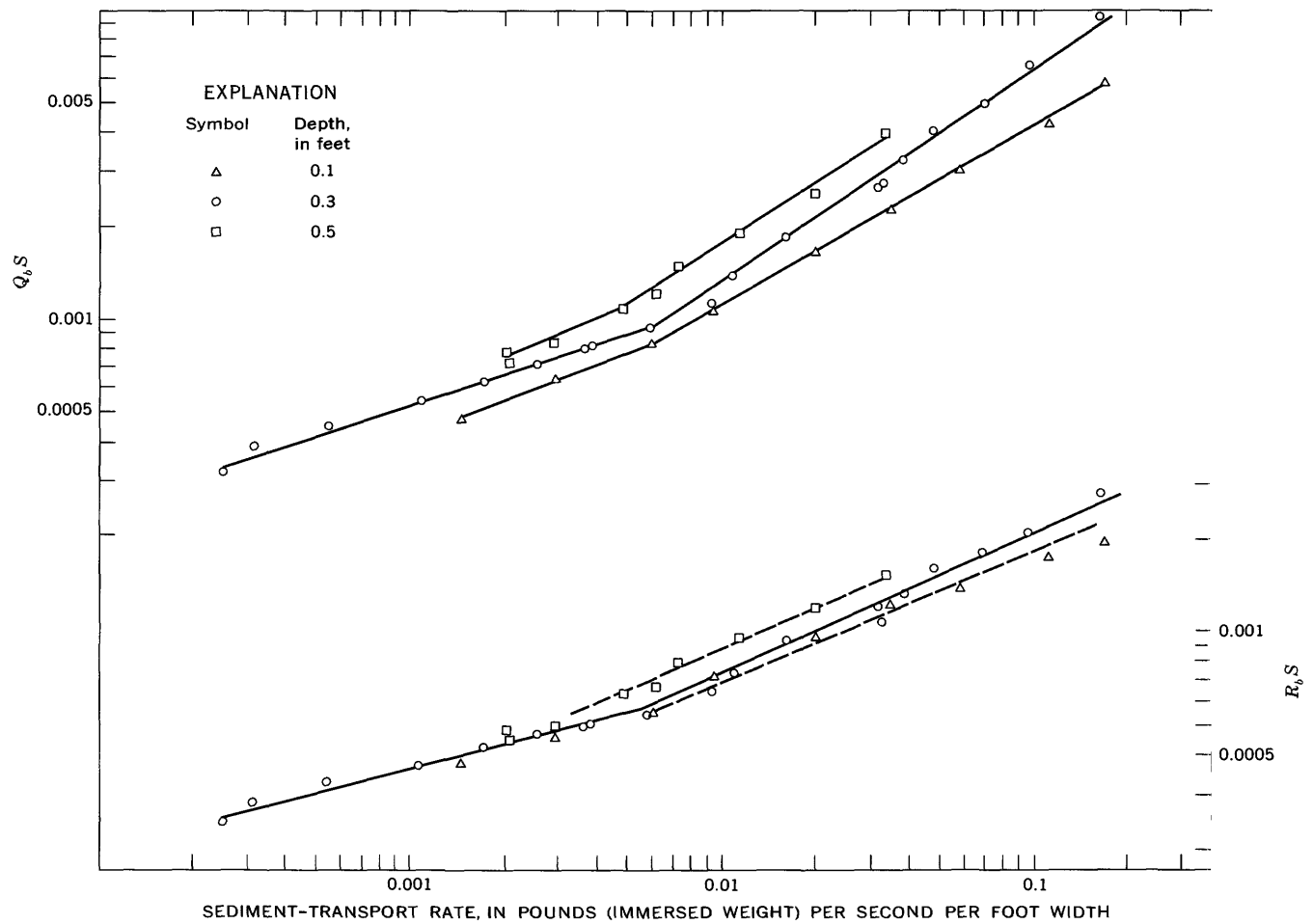


FIGURE 7.—Transport relations adjusted for flume wall drag (Einstein method).

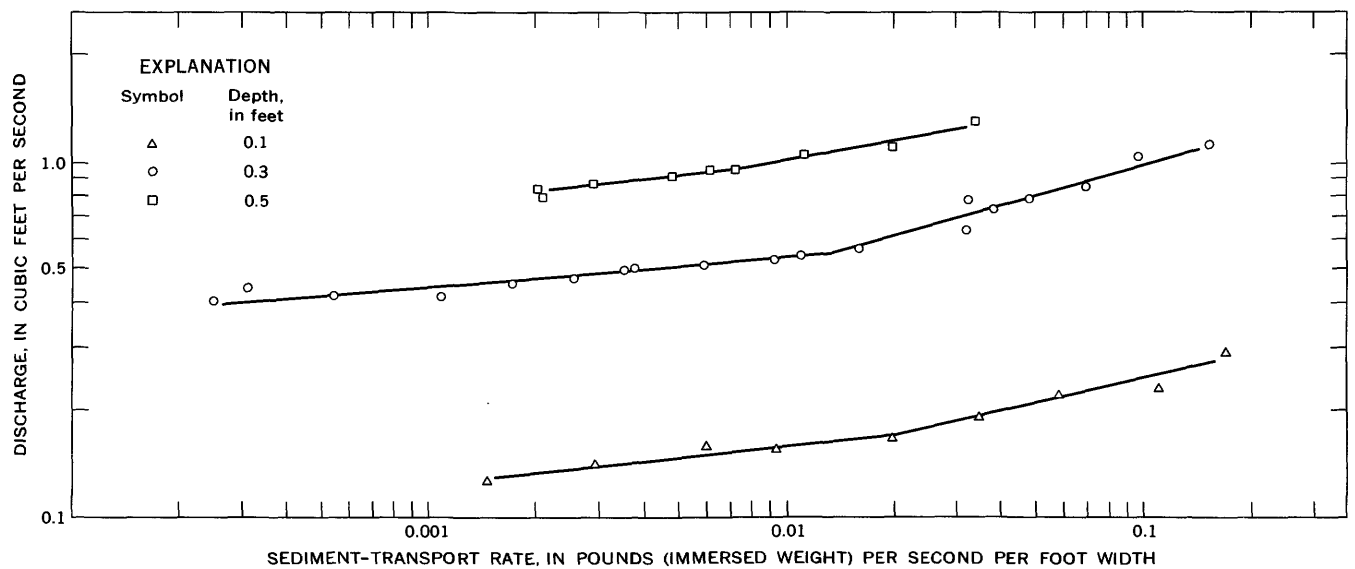


FIGURE 8.—Discharge versus transport relation.

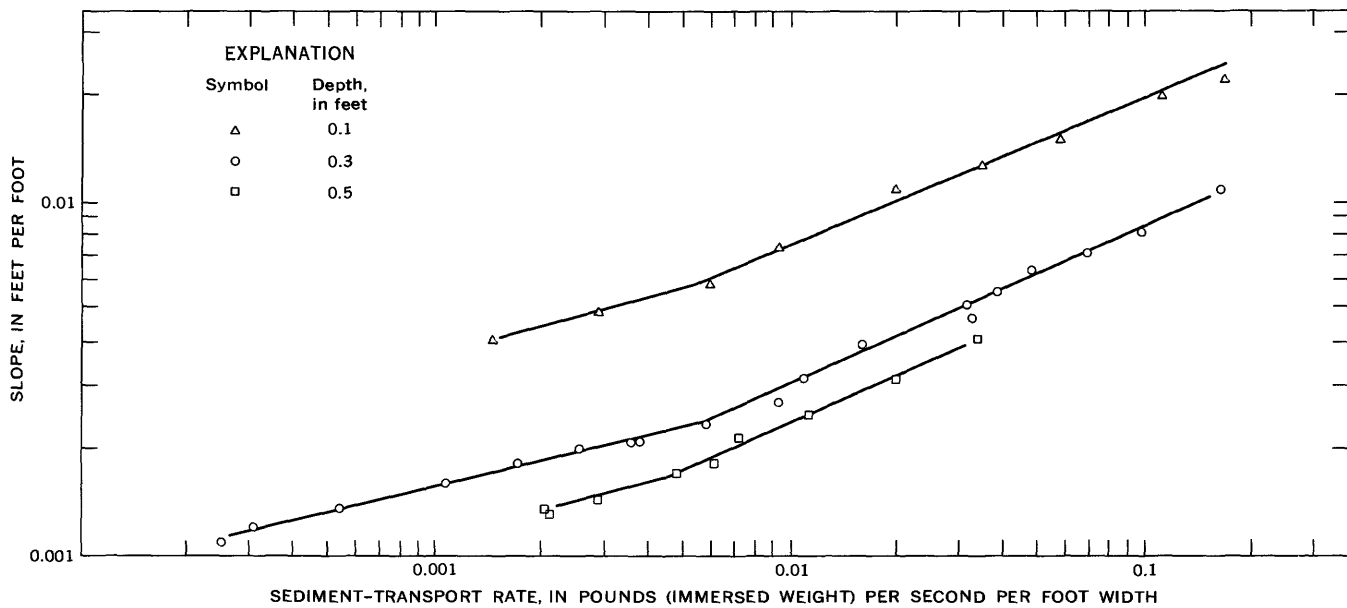


FIGURE 9.—Slope versus transport relation.

seems to suggest the presence of two regimes. At low sediment-transport rates, slope was approximately proportional to  $i^{0.26}$ . At transport rates greater than about 0.06 lbs per sec per ft the relation changed to approximately  $S \propto i^{0.43}$ .

The reason for the break in the  $Q/i$  and  $S/i$  relations is unknown. The same break was noticed in the diagrams relating flow strength to transport rate (figs. 2-6), all of which involve either or both  $Q$  (or components of  $Q$ ) and  $S$ .

The resistance to flow was computed using the three common measures currently in use: Chezy  $C (=V/\sqrt{RS})$ , Manning  $n (=1.486 R^{0.67} S^{0.50}/V)$ , and Darcy-Weisbach  $f (=8gRS/V^2)$ . The calculated values (table 2) indicate that the resistance to flow did not change much within the range of conditions investigated; a rather slight increase in resistance occurred with increasing sediment-transport rates.

Unique relations were also found between slope and water discharge, and therefore between slope and velocity, for a given depth (fig. 10). (For a constant depth and flume width, velocity varies directly with discharge.) Slope increased about as the 2.5 power of water discharge or velocity. Other investigators, however, have reported different findings. Brooks (1958) and Vanoni and Brooks (1957) found that when bed forms (dunes) began to be swept away during the transition to plane-bed stage, the  $S/V$  trend for a given depth was reversed so that an increase in velocity was accompanied by a reduction in slope. This reversal was possible because of the decrease in flow resistance resulting from the gradual disappearance of the bed

forms. After the plane-bed stage was attained in the studies just cited, slope stopped decreasing and began increasing again with further increase in velocity. The resulting  $S/V$  curves thus showed that more than one velocity was possible for a given slope and depth within a certain range of bed configurations. The absence of any such break in the present curves leads to the question of what differences existed in the two groups of experiments.

The chief differences seem to be that Brooks and Vanoni used relatively fine grain sizes (about 0.08–0.15 mm median diameter), recirculating flumes, flumes having dimensions different from the present flume, and dependent and independent variables differing from those of the present study. Flume dimensions seem to be the least significant factor because two flumes were used in the Brooks and Vanoni work (flume A was 10.5 in. wide  $\times$  40 ft long and flume B was 33.5 in. wide  $\times$  60 ft long) and the present apparatus is intermediate in size between these two flumes. Little information is available to indicate that differences should be expected in data obtained in recirculating versus nonrecirculating flumes. In both groups of experiments depth was an independent variable. Sediment-transport rate, however, cannot be an independent variable in a recirculating flume; discharge (and consequently, velocity) was independent in the Brooks and the Vanoni-Brooks studies. The same relations between variables might be expected to exist regardless of which factors were dependent and which were independent during the runs. The ranges of flow conditions were comparable for the two groups of experiments.

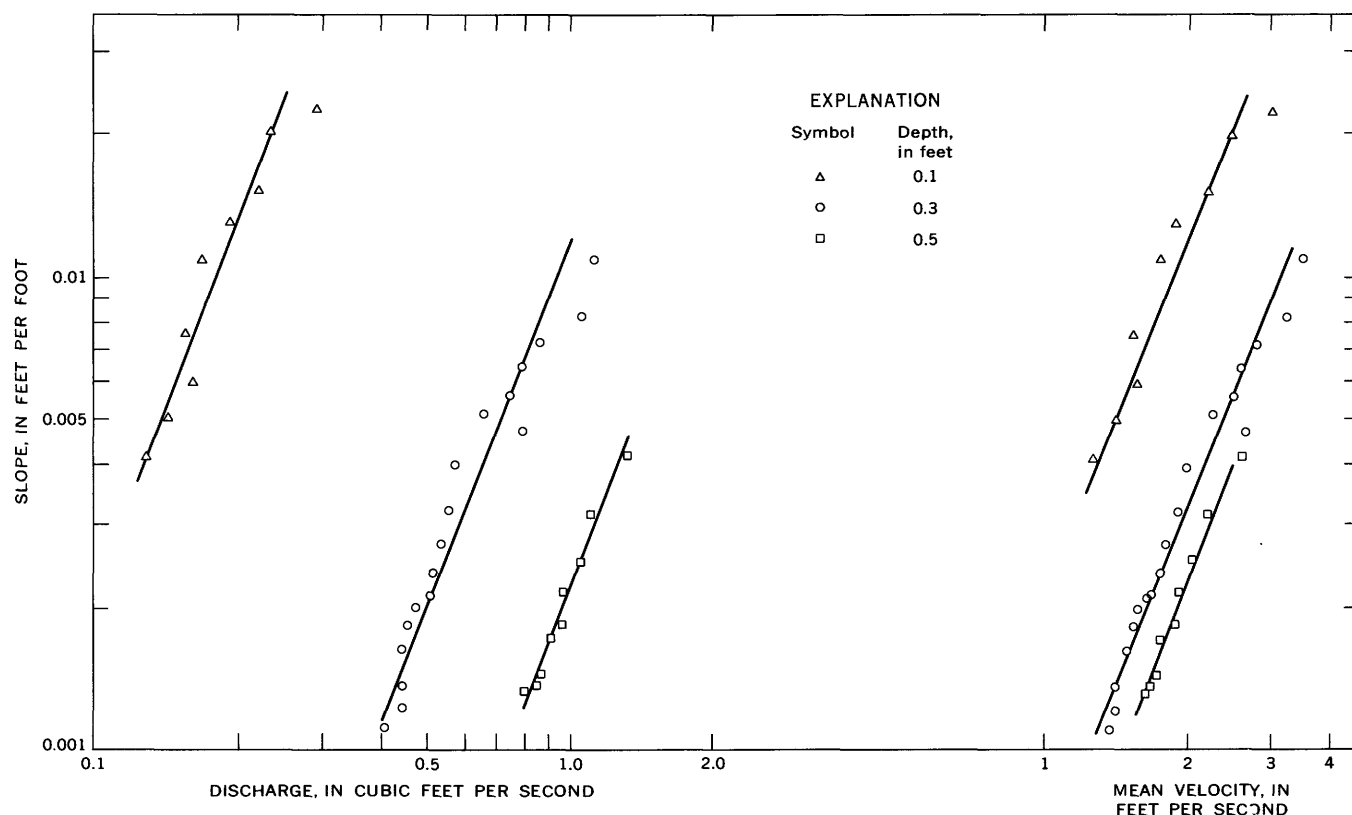


FIGURE 10.—Relations of slope to discharge and mean velocity.

The most likely cause of the differing results in the slope-velocity trends would seem to be the grain size and the associated differences in bed behavior. With the relatively large grains used in the present experiments, the bed forms gradually progressed from dunes directly to antidunes. Bypassed completely were the transition from dunes to plane-bed stage and the plane-bed stage (at least at the greater depths), where the reversal of the  $S/V$  trend occurred in the Brooks and Vanoni-Brooks tests. As pointed out by Simons, Richardson, and Nordin (1965a), with coarse sand and shallow depths the dune stage may not terminate until the Froude number is so large that the subsequent bed form is antidunes instead of plane bed. In the absence of transition and plane-bed stages similar to those that occurred when finer grain sizes were used, no marked reduction in flow resistance occurred in the present runs, and the mean velocity increased consistently with increase in slope.

In summary, the measurements made in this investigation indicate that as soon as depth and any other variable (except flow resistance) were chosen, the values of all other variables were uniquely determined. (The value of flow resistance could also be ascertained because resistance is uniquely determined once  $D$ ,  $S$ , and  $V$  are

determined.) The merit of depth as an independent variable in flume studies perhaps deserves emphasis. When depth is kept constant, the relations among variables appear to be much more clearly defined.

#### SURFACE VELOCITY

Surface velocities were measured only to provide an approximate check on the mean velocity. Inspection of the data, however, reveals some consistent relations involving surface velocity.

The relation between surface velocity ( $V_s$ ) and rate of sediment transport in the present experiments was surprising (fig. 11), because the influence of depth was virtually eliminated. Except in the  $\gamma RS/i$  plot, an elimination of the depth effect did not occur with the other measures of flow strength related to sediment transport (figs. 2-6). Therefore, in the present study, the easiest and quickest method of estimating sediment-transport rate was a simple measurement of surface (float) velocity. Furthermore, the point scatter in figure 11 is small enough that any estimate of  $i$  using  $V_s$  would be reasonably accurate.

The variation between mean velocity and surface velocity for the various depths investigated is shown in figure 12. The  $W/D$  ratio is used on the abscissa

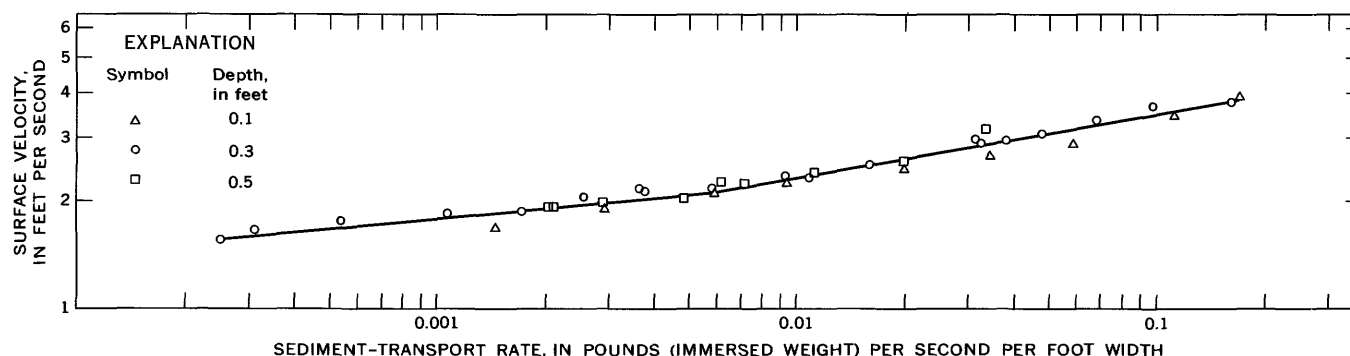
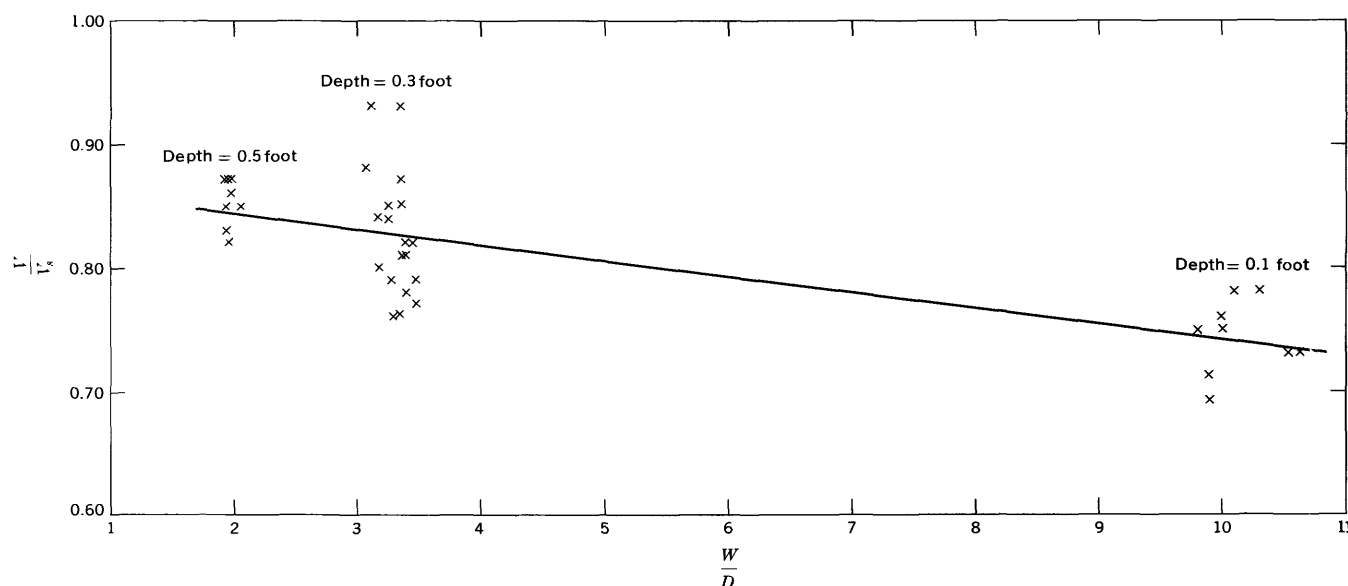


FIGURE 11.—Surface velocity versus transport relation.

FIGURE 12.— $V/V_s$  relation for various depths.

although width was constant throughout. Average  $V/V_s$  values as indicated by the line of best fit are 0.85, 0.83, and 0.74 for depths of 0.5, 0.3, and 0.1 foot, respectively. The  $V/V_s$  ratio is thus seen to decrease with depth by a very small increment, so that  $V_s$  departs farthest from  $V$  at a very shallow depth. For the present runs, use of the approximations would introduce possible  $V/V_s$  errors of about 3.0, 12.0, and 7.0 percent for the 0.5-, 0.3-, and 0.1-foot depths, respectively.

Figure 12, then, shows the proportionality that exists between  $V_s$  and  $V$  for a given depth (or  $W/D$  ratio). A fixed proportionality also exists between  $V_s$  and  $Q$  for a given depth, as might be expected (fig. 13A). Since  $Q$  varies directly with  $V$  for a constant depth and width,  $Q$  also varies directly with  $V_s$ .

The relation between surface velocity and slope is shown in figure 13B. If the plot of slope as a function of mean velocity were transferred for comparison

purposes to figure 13B, it would be clear that the surface-velocity versus slope proportionality is exactly the same as that between mean velocity and slope, as would be expected. This relation is  $V_s \propto S^{0.41}$ .

In summary, the surface velocity in this study was consistently related to all the other variables. Consequently, use of surface velocity may be an aid in determining the values of other variables, at least within the range of conditions examined here. Surface velocity is obviously easier to measure, and, for the present data, its relation to other variables is dependable.  $V_s$  alone can provide a reasonably good appraisal of both sediment-transport rate and mean flow velocity. When water depth is also known,  $V_s$  could be used to uniquely determine the slope and the discharge. Thus, such factors as power and shear also are uniquely related to surface velocity, for a given depth.

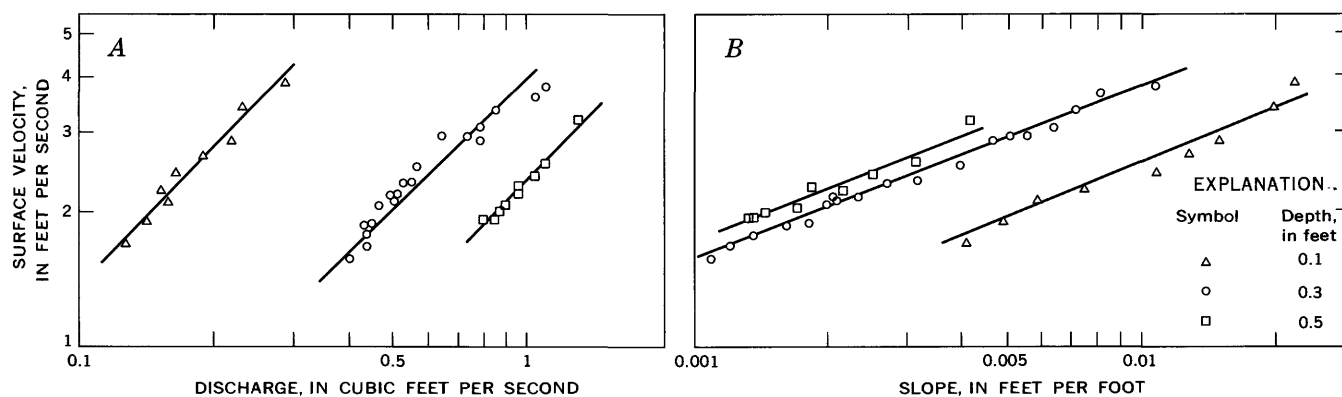


FIGURE 13.—Relations of surface velocity to slope and discharge.

The surface-velocity relations may never be well defined for many natural-stream situations, owing to the complexities of these situations, nor for other laboratory investigations. However, sufficient information is not yet available to negate the possibility that reliable relations exist. In future laboratory and field studies, it may be worthwhile to measure surface velocity and see what relations exist between it and the other variables.

#### COMPARISON WITH DATA OF GILBERT AND MURPHY

In this section the data from the present investigation are compared with the Gilbert-Murphy data (Gilbert, 1914) for their grade E, a comparable grain size (0.84–2.00 mm, nominal diameter 1.71 mm). With this grain size Gilbert and Murphy used flume widths of 0.66, 1.00 and 1.32 feet, and depths ranging from 0.077 to 0.562 foot. In the present comparison, all their grade E data have been included regardless of widths and depths. Their results have been computed for unit flume width, and their transport rates (dry weight) have been converted to immersed weight by the relation  $\text{immersed weight} = \frac{2.65 - 1.00}{2.65} \times \text{dry weight} = 0.624 \times \text{dry weight}$ . Depth was not controlled in the Gilbert-Murphy experiments; transport rate and discharge were the independent variables. Most of their runs were made at the higher transport rates.

The stream-power versus transport relation, on which the depth influence would be expected to appear, is shown in figure 14. The Gilbert-Murphy points are represented by dots, and the water depth is given beside each dot. For comparison, the lines for each depth from the present study are also included. In a general way the depth effect is discernible from the plotted points, and it is perhaps more noticeable at higher sediment-transport rates. It would be difficult, however, to sketch in lines of constant depth for the Gilbert-Murphy data. In other words, the Gilbert-

Murphy points occupy the same band on the graph as do the points for the present data, but the points for the present data reveal the influence of depth much more clearly.

Because all the present runs plot on a single line if shear ( $\gamma RS$ ) is used as the measure of flow strength, a graph of the  $\gamma RS/i$  relation was also prepared (fig. 15). On this plot the point scatter of the Gilbert-Murphy data is so reduced that the depth can not be labeled beside each point, and symbols are used to represent depth ranges. The depth effect is eliminated, as in the present data, but there is slightly greater point scatter in this plot than in the plot of the present data (fig. 4). The line of best fit for the present data is reproduced in figure 15; the agreement with the Gilbert-Murphy data is very good.

The relations among mean velocity, depth, slope, and resistance to flow in the two sets of experiments can be seen from a plot of  $V$  versus  $DS$  (fig. 16);  $DS$  is, of course a measure of shear. A straight line on log-log scales can be fitted to both sets of data, indicating the existence of a power function, similar to the Chezy equation of the form

$$V = a(DS)^b.$$

Closer inspection shows that the two fitted lines duplicate each other. The fact that both sets of data are identical indicates that for the two investigations (a) the relation of velocity to shear is identical, and (b) the relation of flow resistance to velocity and shear is identical (resistances are the same). The actual definition of resistance is irrelevant.

The value of the exponent  $b$  is about 0.42. For values of  $b < 0.50$ , resistance to flow increases with increasing shear or mean velocity. The very slight increase of flow resistance with increasing shear or mean velocity, as indicated by the value of  $b$ , can be seen from the trend in the computed resistance (table 2).

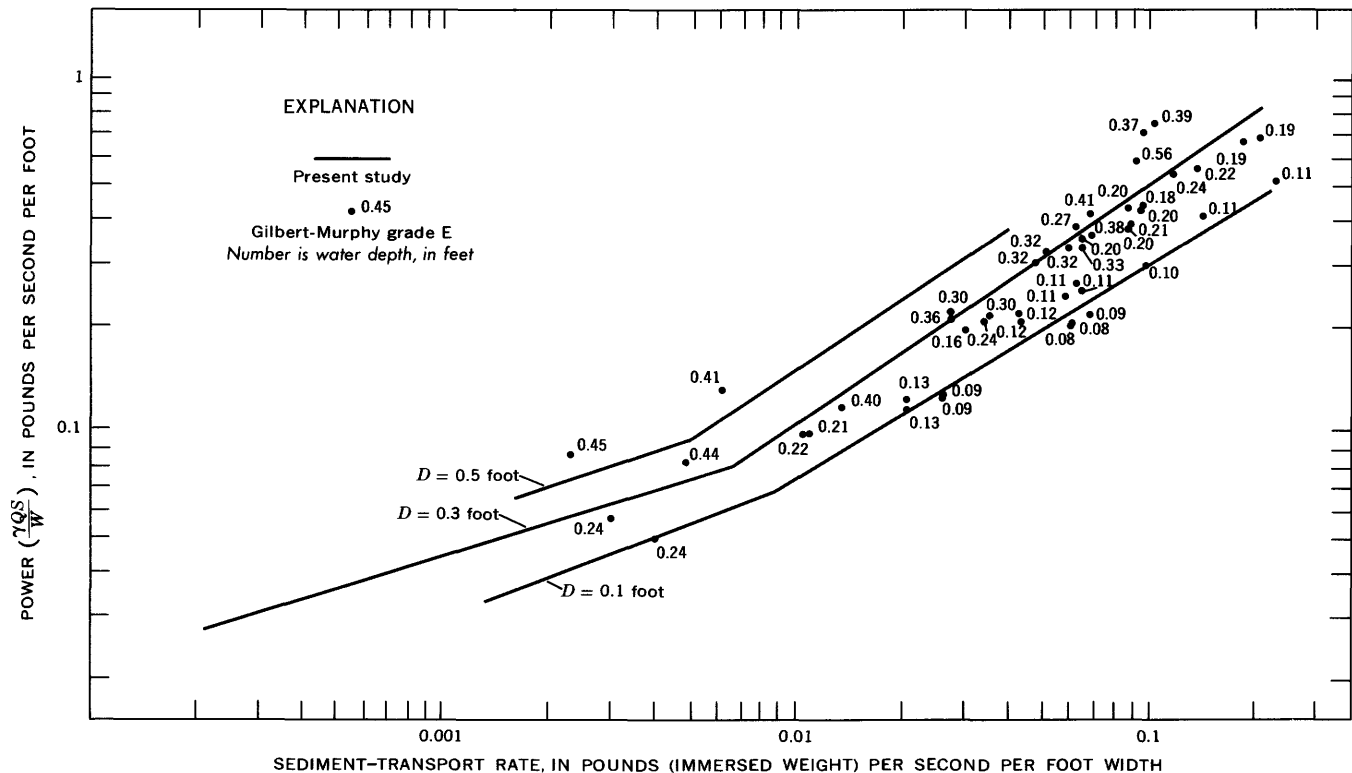


FIGURE 14.—Comparison of stream power versus transport relations with data of Gilbert and Murphy.

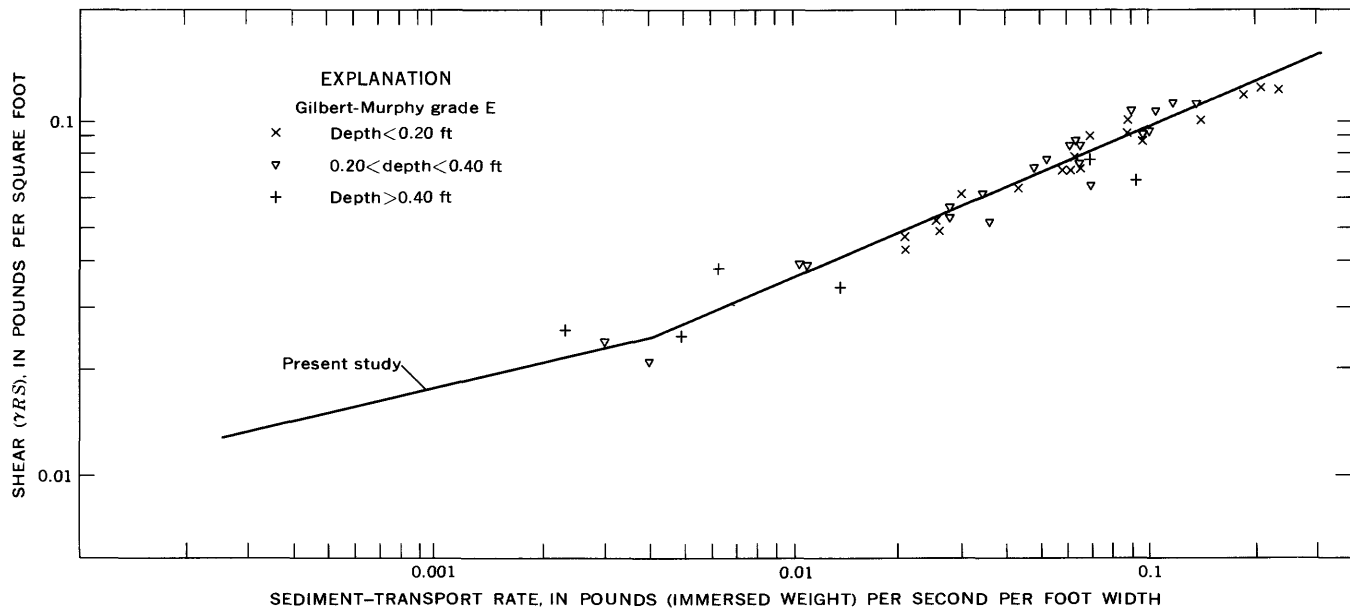


FIGURE 15.—Comparison of shear versus transport relation with data of Gilbert and Murphy.

The general agreement between part of the Gilbert-Murphy work and the present study is perhaps significant, for it indicates that some of the Gilbert-Murphy data are reproducible. Several details of experimental equipment and procedure differed in the two investigations, but, these differences apparently did not greatly affect the experimental results. For example, in the

Gilbert-Murphy work on stream traction using grade E sand:

1. Two different flumes were used. One of these had a length of 24.5 feet from sediment infeed to sediment catchment (31.5 ft, overall), and the other had an overall length of 150 feet. (The present study employed a 52-foot-long flume.)



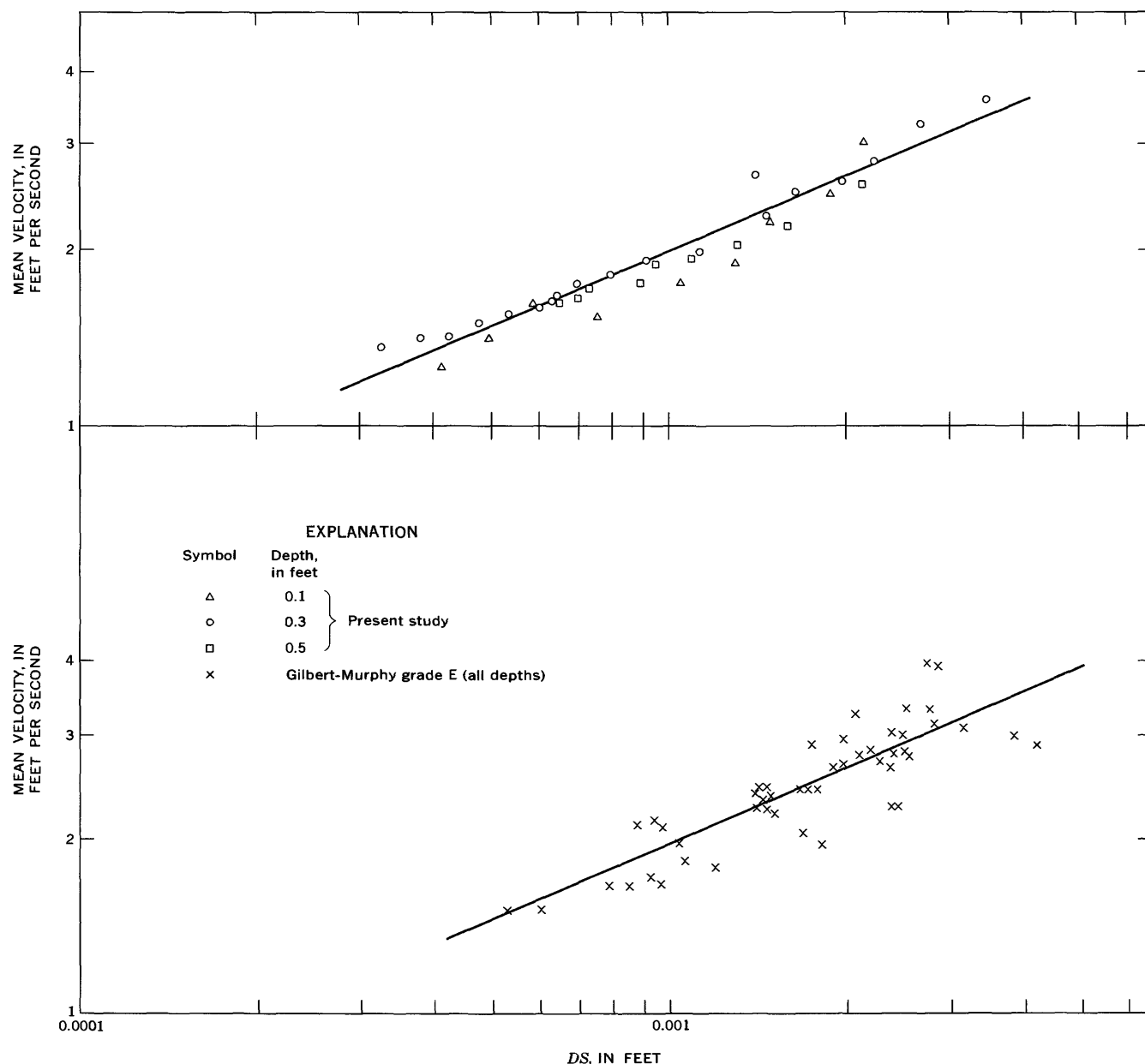


FIGURE 16.—Mean velocity versus shear ( $DS$ ) relations compared with data of Gilbert and Murphy.

2. Various flume widths were used.
3. Depth was not controlled—transport rate and discharge were the independent variables.
4. The flume was horizontal and was devoid of sand at the beginning of each run; that is, slope was not estimated and not preset.
5. The method of sediment infeed was different from the present study. Sand was dropped into the stream from above—usually by hand (by dumping in a boxfull at timed intervals), but occasionally by a hopper (at low transport rates).
6. Transport rate was measured during a relatively short period.

7. Sediment-infeed rate did not always equal the collection rate.

Some of the above features might account for some point scatter in the Gilbert-Murphy data.

#### BED FORMS

For sediment finer than 0.6 mm in median fall diameter, the usual sequence of bed forms produced in flume studies by increasing stream power was defined by Simons, Richardson, and Nordin (1965a) as ripples, ripples on dunes, dunes, transition, plane bed, antidunes, and chutes and pools. For material coarser than 0.6 mm they reported that the ripple and ripple-

on-dune stages are absent, and that the transition and plane-bed stages may or may not occur.

The types of bed configuration produced in the present study by increasing stream power were plane bed (at extremely low sediment-transport rates), dunes (at depths of 0.3 and 0.5 ft), and antidunes. A description of the bed configuration for each run is given in the section starting on p. B28. The initial flat-bed stage appeared to be relatively unstable, as extremely low crests (probably incipient dunes) occasionally formed at a few locations during the first run ( $D=0.3$  ft). At very low sediment-transport rates, definitive bed forms appeared. These first bed forms were different in runs at the 0.1-foot depth than in runs at greater depths.

At a depth of 0.1 foot, the run at lowest stream power produced an almost flat bed. With increase in flow strength (and hence in transport rate) a peculiar bed feature appeared that was a few grain diameters high. Such a bed form, herein called a meandering scar, began at the flume wall and curved toward the center of the channel downstream (fig. 17). It usually faded out completely in the middle of the channel. The adjacent bed feature, a mirror image of its neighbor, would begin from the opposite wall a short distance downstream from the first feature. (Similar features also were found under certain conditions after the water had been drained from the flume.) With further increase in flow strength the meandering scars disappeared except in the downstream part of the flume (run 4). At the same time (run 4) symmetrical antidunes of very low amplitude appeared throughout most of the flume, though present only in the center of the channel in a single row. The distinguishing feature of antidunes is an inphase relation between sand crests and water-surface crests. These initial antidunes had wavelengths of about 0.5 foot. In subsequent runs the meandering scars disappeared entirely and only antidunes were present. With continued increase in flow strength, two or possibly three rows of antidunes occurred side by side in the flume simultaneously. Adjacent lines of these bed forms had staggered sand crests and troughs, so that a checkerboard pattern formed. Some rhythmic periodicity occurred in the formation and disappearance



FIGURE 17.—Pattern of typical meandering scars.

of water surface irregularities (waves). At the highest flow strength examined at 0.1-foot depth, the antidunes were mostly flattened out, and so was the water surface. This rather flat bed was only occasionally interrupted by a short train (3–10 ft long) of antidunes, moving downstream. All the antidunes traveled downstream.

At depths of 0.3 and 0.5 foot, dunes were the initial bed configuration (except in the first run at 0.3-ft depth, during which the bed remained flat). The distinguishing characteristic of dunes as opposed to antidunes is an out-of-phase relation between the sand crests and the water-surface crests. (Ripples are generally less than 1 ft in wavelength, and the present features had an average minimum wavelength of 1.5 ft). These dunes were noticeably asymmetrical from a side view; they were characterized by a long upstream side, a crest which varied from angular to somewhat rounded with increasing flow strength, and a relatively short and steep downstream face. At low transport rates the upstream face was extremely long, in comparison with the downstream face, and the downstream face seemed to be about at the angle of repose. The spacing of well-defined crests under these conditions was somewhat irregular downstream, and the crests were usually perpendicular to the flume walls and extended across the whole channel. As flow strength was increased, three particular changes were observed in the dunes: (a) the length of the upstream face progressively decreased, and that of the slip face increased; (b) the angle of the slip face tended to decrease as the sand grains began to be propelled down the slip face rather than sliding down under their own weight; and (c) the angle between the dune crests and the flume walls changed—though still extending from wall to wall, the crests began assuming irregular and curving fronts and reached the opposite wall 1 or 2 feet farther downstream from their origin. Furthermore, the water surface became increasingly irregular. (At  $D=0.5$  foot the maximum flow capacity of the flume was reached, while the dunes were beginning to be inclined to the walls and were showing some irregularity in crest directions.)

The characteristics just described probably represent a transition from dunes to antidunes. This transition evolved gradually; no tendency to develop a plane bed was observed. Clearly defined antidunes, as indicated by an inphase relation between bed and water-surface crests, were recognizable in the final three runs at the 0.3-foot depth. For the complete series of runs at the 0.3-foot depth the bed-form heights and rates of travel consistently increased with increase in flow strength, except, possibly, the travel rates of the antidunes. When antidunes began to form, the water surface be-

came smoother than in the preceding runs and showed rather symmetrical waves. With further increase in flow strength these water-surface waves tended to break occasionally on the upstream side of the wave crest. In the final run the surface waves extended almost completely across the channel and broke with considerable turbulence just upstream from the crest. The antidunes (a) were almost symmetrical from a side view, (b) possessed well-rounded crests that extended across most or all of the channel and were perpendicular to the flume walls, and (c) moved downstream.

With antidunes the water-surface waves and sand waves were not always well developed throughout the flume length; rather, any given segment of the flume would possess well-developed waves during one period, and poorly developed ones during another period. Two or three segments of well-formed waves existed in the flume at any one time; the length of time such a train of well-developed waves persisted ranged from a fraction of a minute to several minutes.

Because of the variations in appearance and measurements of bed forms, the minimum of information which will adequately describe bed conditions must include a description of the features (rather than a single name) in addition to some measurements of bed-form heights, wave lengths, and rates of travel. The characteristics of the water surface must also be noted, especially the phase relation between bed-form crests and water-surface crests. The recording of this information should be a standard practice in flume studies.

During the experiments it became evident that the description and measurement of bed features after the water has drained from a flume should be undertaken only with great caution. No significant difference was found in dune wave lengths during the run and after the run, in those runs for which both measurements were taken. However, bed features existing after the water was drained were frequently quite unlike those that existed during the run. Some examples of feature changes are the following: (a) All antidunes were obliterated as the water left the flume; (b) the general bed-form appearance as well as the heights were often modified as the water drained; (c) whenever the depth was relatively shallow or the bed was somewhat flat during the run, a peculiar type of bed feature (the meandering scars of fig. 17) appeared as the water receded. In many runs the peculiar features did not form until the flume was drained. No sound explanation can be offered for the formation of these features, but the writer suspects that they are associated with deflection of the water by the fixed walls of the flume.

#### INTERRELATIONS BETWEEN CHARACTERISTICS

The rate of bed-form movement (*c*), average bed-

form length (*l*), and average height (*h*) are given in table 4. Heights of well-developed antidunes were generally fairly constant for any given run. The range in dune heights during runs under given flow conditions was small in some runs and several fold in others. The determination of dune lengths was occasionally a subjective procedure. As reported in other studies, dunes under certain conditions are continually dying out, reforming, and overtaking other dunes. In many studies the dunes do not extend very far laterally, and the crests frequently trend diagonally downstream. In the present study, extremely low dune crests which were a few grain diameters high were disregarded. Such incipient bed forms were more common at low sediment-transport rates. In spite of occasional subjectivity in obtaining the values, they should be fairly representative of the prevailing bed forms.

No well-defined relation was obtained between bed-form height and length. The antidunes at  $D=0.1$

TABLE 4.—Bed-form measurements

[No data for runs 1-3]

Run	Height (ft)	Length (ft)		Velocity (ft per sec)
		During run	Dried bed	
<i>C.1-ft depth</i>				
<sup>1</sup> 4-----		0. 5		
<sup>1</sup> 5-----	0. 021	. 5		0. 0200
<sup>1</sup> 6-----	. 042	. 6		. 0216
<sup>1</sup> 7-----	. 083	. 7		. 0300
<sup>1</sup> 8-----	. 053	1. 0		. 0683
<sup>1</sup> 9-----	. 073	. 6		. 0683
<i>0.3-ft depth</i>				
10-----				
11-----	. 021			. 0007
12-----				
13-----	. 042	8. 9		. 0017
14-----	. 042	5. 8		. 0027
15-----	. 053	4. 8		. 0015
16-----	. 063	4. 3		. 0035
17-----	. 042	3. 6		. 0050
18-----	. 053	3. 5		. 0027
19-----	. 053		2. 3	. 0075
20-----	. 053		2. 4	. 0117
21-----	. 063		2. 0	. 0158
22-----	. 073	1. 8	1. 9	. 0267
23-----	. 104	1. 9	2. 0	. 0167
24-----	. 167	1. 3	1. 9	. 0250
25-----	. 125	1. 5	1. 9	. 0384
26-----	. 167	1. 5		. 0083
27-----	. 250	1. 6		. 0400
28-----	. 250	1. 6		. 0350
<i>C.5-ft depth</i>				
29-----	. 083	5. 2	4. 6	. 0012
30-----	. 042	3. 9	4. 6	. 0007
31-----	. 104	3. 7	3. 5	. 0017
32-----	. 063	2. 8	3. 0	. 0018
33-----	. 042	2. 9	2. 7	. 0022
34-----	. 063	2. 5		. 0020
35-----	. 167	2. 0	2. 2	. 0072
36-----	. 167	2. 2	1. 8	. 0063
37-----	. 167	1. 8	1. 8	. 0217

<sup>1</sup> Antidunes.

foot tended to increase in height as their length increased, but dunes increased in height as length decreased. Height and length relations alone could not distinguish dunes occurring at a depth of 0.3 foot from those occurring at a depth of 0.5 foot.

The data further indicate that bed-form height increased as rate of travel increased. The relation between either height or wavelength and bed-form velocity serves to distinguish the runs roughly on the basis of flow depth. Although the point scatter precludes a precise relation, figure 18 suggests that for a given dune height the rate of movement downstream is slower at a greater depth. The wavelength versus bed-form velocity relations (fig. 19) show that as dune velocities increased the wavelengths gradually decreased, apparently reaching a limiting minimum value of about 1.5 foot. The wavelengths of the antidunes at  $D=0.1$  foot generally increased as bed-form velocity increased.

#### CHARACTERISTICS RELATED TO FLUID FLOW STRENGTH

When antidunes at depths of 0.1 and 0.3 foot became clearly recognizable, the Froude number, representing the ratio of inertial to gravity forces, was about the same for both depths ( $F \approx 0.85$ ). The value of the fluid flow strength was considerable greater, however, at a depth of 0.3 foot at the onset of formation of antidunes. The antidunes at the two depths had somewhat

different characteristics; at the 0.1-foot depth they were much smaller in size, more symmetrical in all directions, and usually did not exist near the flume walls. Also, trains formed side by side in runs at a depth of 0.1 foot, but not at a depth of 0.3 foot.

Prior to the antidune stage, dunes existed at depths of 0.3 and 0.5 foot but not at a depth of 0.1 foot. Furthermore, the dunes at the two greater depths were rather similar in appearance. This similarity, in contrast to the complete absence of dunes at the shallowest depth, seems rather suggestive of a depth effect on type of bed form. Unless wall drag or some other factor had a great influence on the bed forms which occurred in these experiments, it appears that the depth of flow caused substantial differences between bed forms occurring at the shallowest depth and bed forms of the two deeper depths. Apparently, somewhere between the 0.1 and 0.3-foot depths a critical depth existed below which the bed features, especially dunes, were greatly inhibited in their formation by shallow depth. Thus, flow depth may place certain limitations on bed-form characteristics. The existence of these limitations, such as on maximum attainable heights of bed forms, has been suggested by various investigators.

#### Height

In figure 20 the average height of the bed forms is plotted against mean velocity, surface velocity, shear,

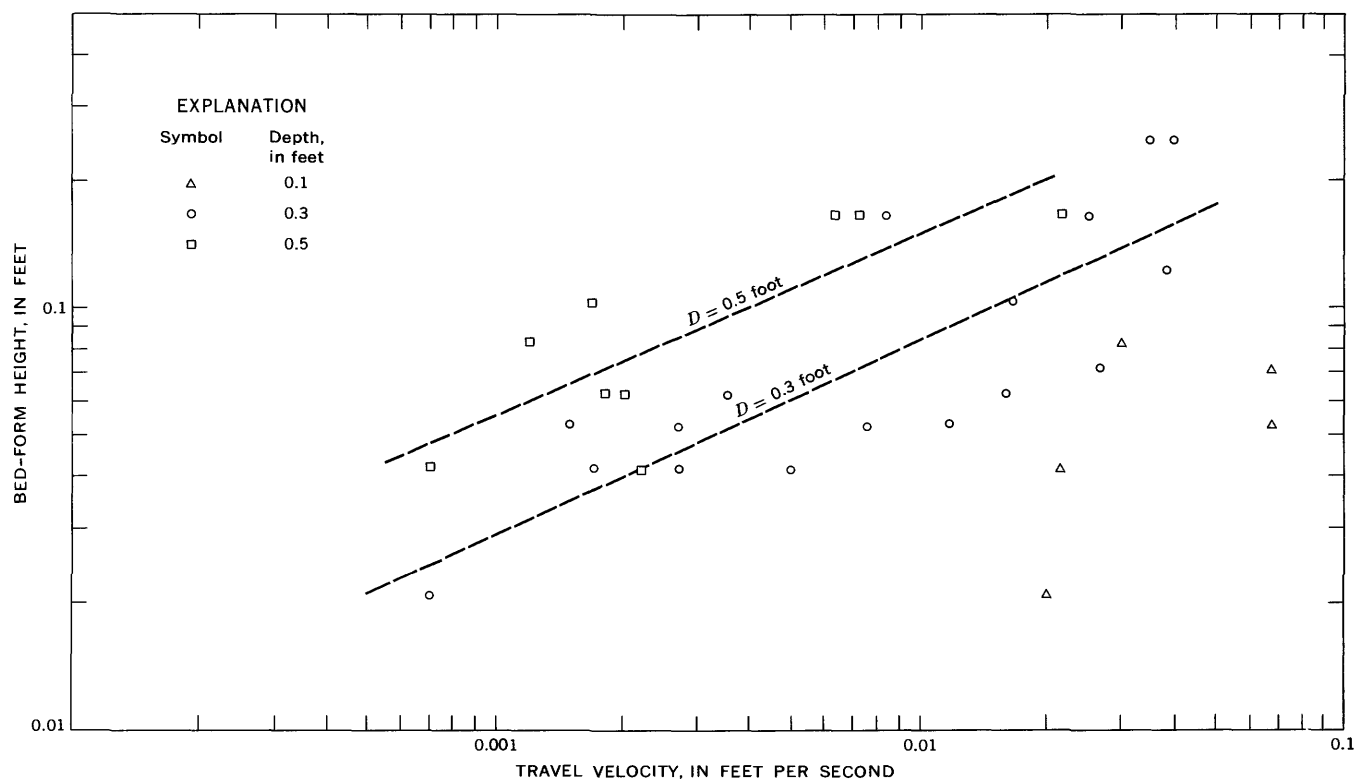


FIGURE 18.—Variation in bed-form height with travel velocity.

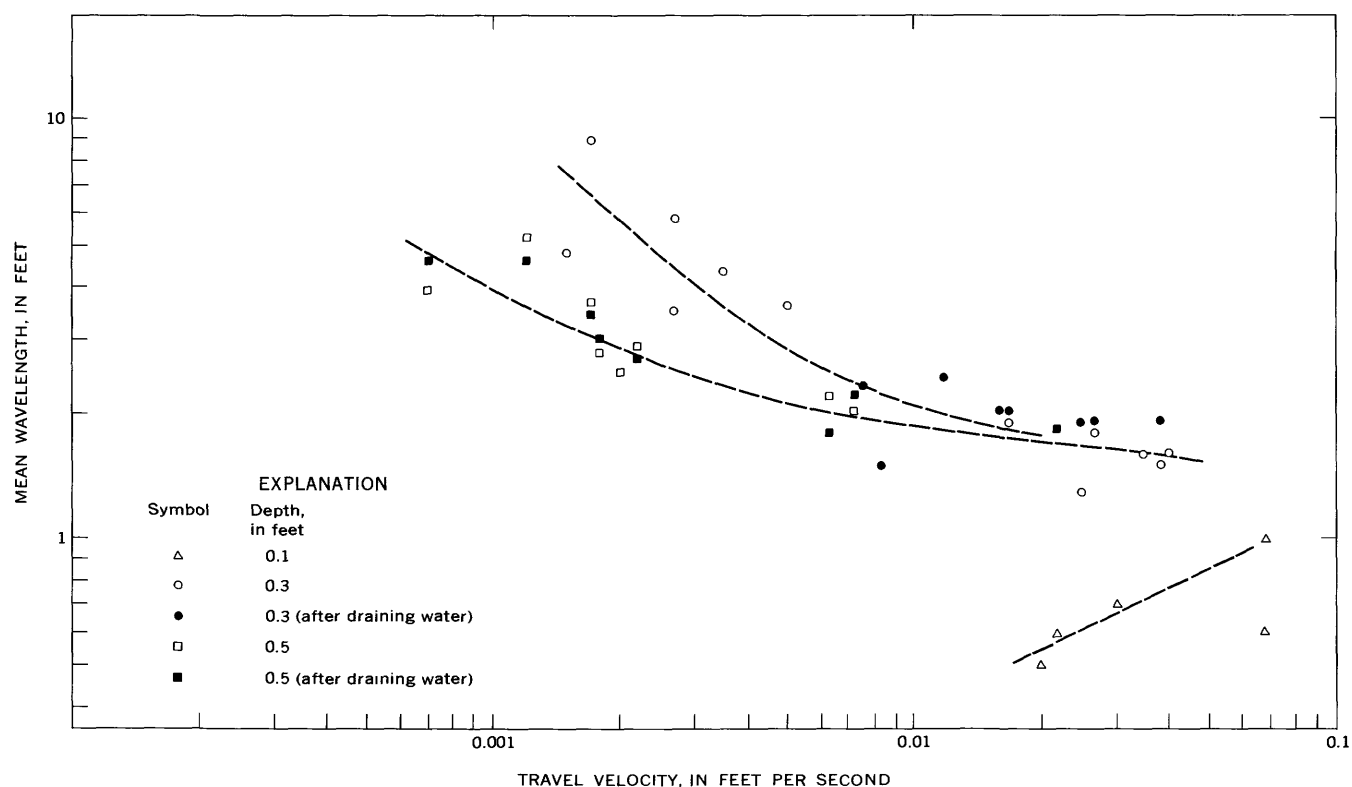


FIGURE 19.—Variation in bed-form wavelength with travel velocity.

and power. (The constant  $\gamma$  is dropped in the computation of shear and power. The fitted lines do not include the antidunes at  $D=0.1$  ft.) The heights of the bed features increased progressively with increase in flow strength. Dune heights grew with about the 3.2, 3.2, 1.2, and 0.9 powers of mean velocity, surface velocity, shear (either definition), and power, respectively. The antidunes at  $D=0.1$  foot differed from the bed forms at greater flow depths whose heights were greater for a given flow strength. In spite of the point scatter, there is no clear indication (except possibly with the  $V_s$  plot) that the heights of the dunes occurring at the 0.3-foot depth were significantly different from those at the 0.5-foot depth.

#### Length

The relation of mean wavelength to each of the measures of flow strength is shown in figure 21. The antidunes that formed at the shallow flow depth had short intervals and are separated from the other bed forms. Also, the lengths of these antidunes increased, whereas those of the dunes decreased, as flow strength increased. The curves indicate that a fair estimate of flow strength could be obtained from a determination of mean dune wavelength. The antidunes that formed at a depth of 0.3 foot (the last few runs) did not show any significant change in wavelength with increase in fluid flow strength. For a given flow strength, a change

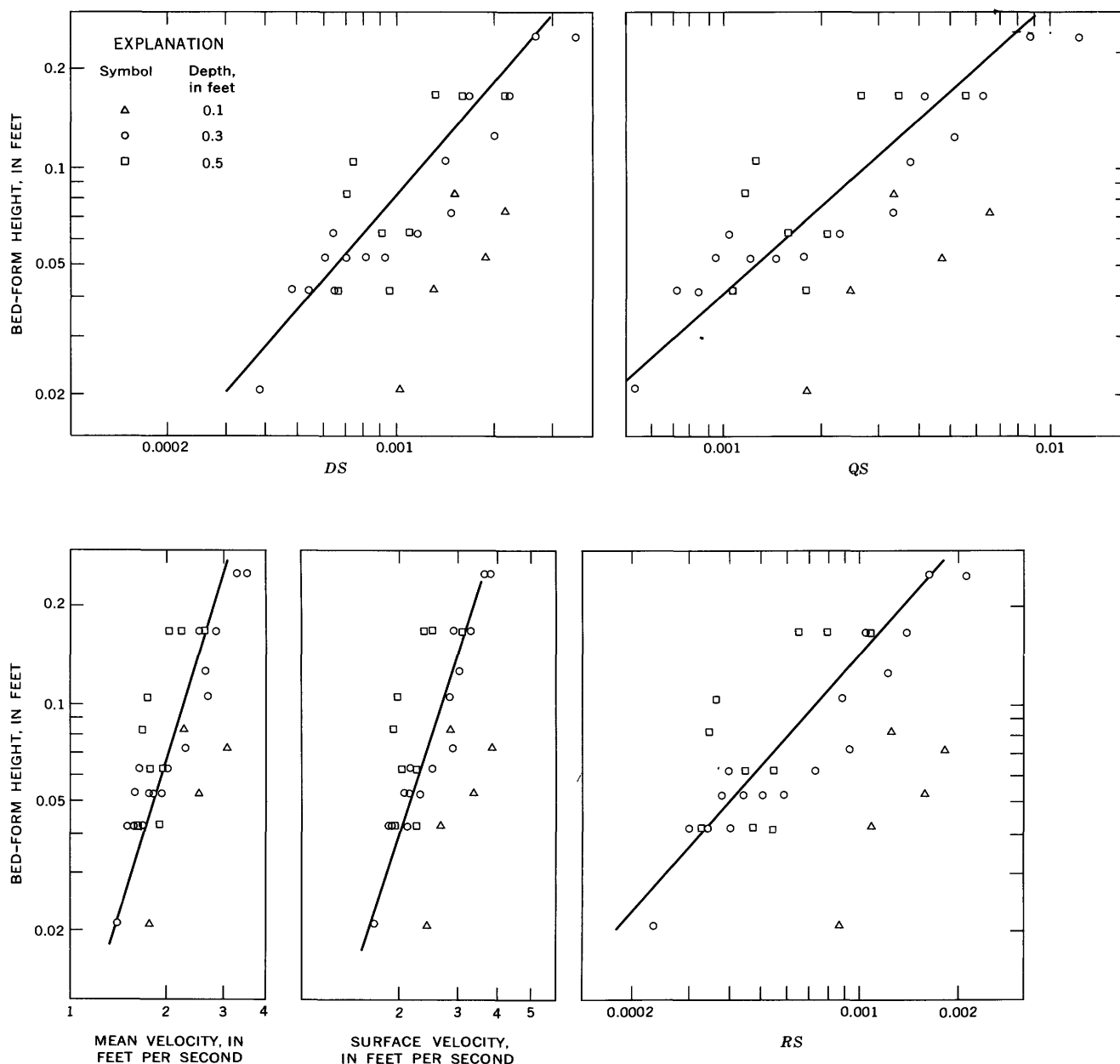
in depth from 0.3 to 0.5 foot apparently did not affect the mean dune wavelengths.

#### Velocity

The relation of rate of bed-form travel to the various measures of flow strength is presented in figure 22. The velocity of the bed features increased with greater flow strength. A slight increase in flow strength caused a relatively large increase in rate of bed-form movement. The rate of bed-form travel varied approximately with  $V^{7.2}$ ,  $V_s^{7.2}$ ,  $(RS)^{2.6}$ ,  $(DS)^{2.2}$ , and  $(QS)^{1.5}$ . Liu found in certain flume experiments using finer sand that bed-form velocity is proportional to  $V^5$ .

The depth effect can be distinguished on the  $DS$  and  $QS$  diagrams. As indicated earlier on the sediment-transport diagrams (figs. 2, 3), the amount of sediment transported, at a given  $DS$  or  $QS$  value, increased as the water depth decreased, within the range of flow conditions studied. Figure 22 is consistent with this trend; it shows that the bed forms moved downstream faster as depth decreased when  $DS$  and  $QS$  were the measures of flow strength.

As can be seen in the diagrams, the lines for the various depths are farthest apart on the power plot. They are closer together on the  $DS$  diagram, and the plots of bed-form velocity versus  $RS$ ,  $V$ , and  $V_s$  practically eliminate the effect of depth.

FIGURE 20.—Bed-form height versus measures of flow strength. (Lines exclude  $D=0.1$  ft.)

## CHARACTERISTICS RELATED TO SEDIMENT-TRANSPORT RATES

The general trend of bed-form measurements with increase in transport rate can be seen in table 4. The bed-form length versus transport relation is virtually the same as that shown by the plots of wavelength versus flow strength. Bed-form height increased consistently with increase in transport rate (fig. 23). The point scatter precludes, and indeed the accuracy of the height values does not warrant, an attempt to fit an extremely accurate line to the data. The approximate relation for the bed forms at depths of 0.3 and 0.5 foot is  $h \propto i^{0.40}$ . The same remarks also apply to the

bed-form velocity versus transport diagram (fig. 24), where the general relation is about  $c \propto i^{0.76}$ . Bed-form heights, wavelengths, and velocities are frequently not constant from one bed form to the next, within a given run. In both the  $h/i$  and  $c/i$  diagrams there is a faint suggestion that if more accurate means of measurement were available it might be possible to draw a separate line for each flow depth.

The bedload equation proposed by Simons, Richardson and Nordin (1965b), based on ripple and (or) dune heights and rates of travel, was tested on the present data. The authors cited used the equation for sand ranging from 0.19 to 0.93 mm in median fall diameter.

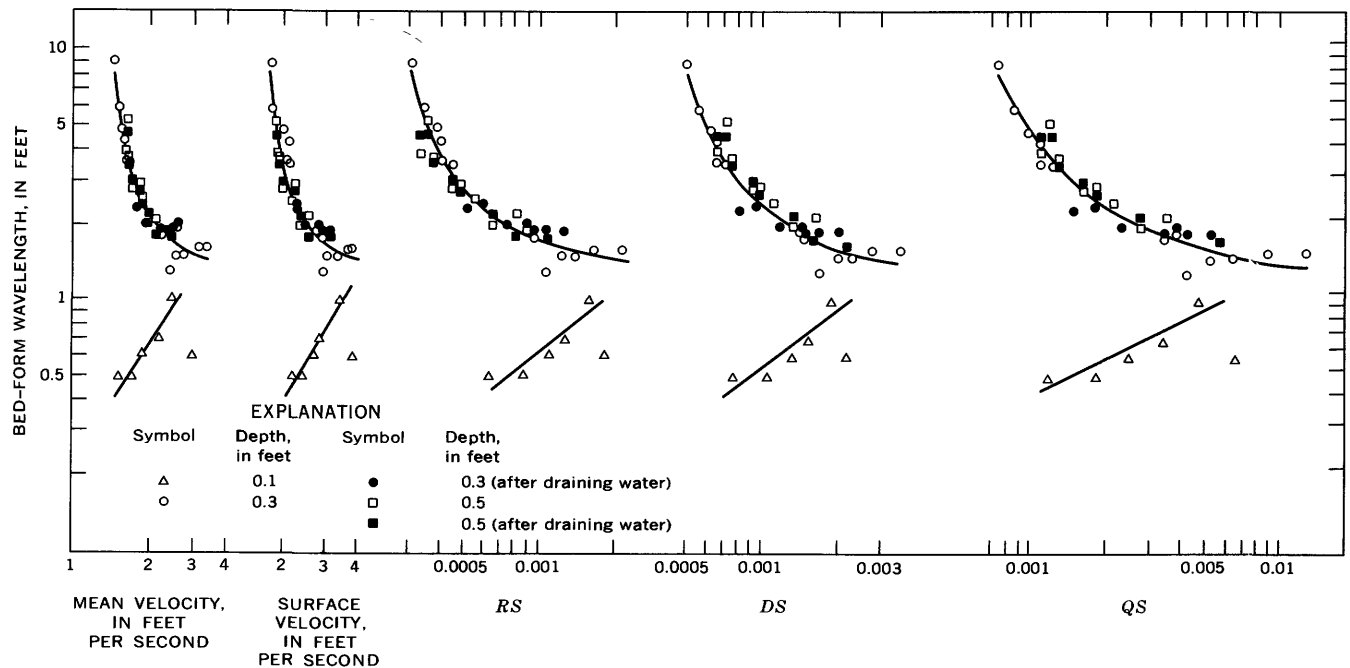


FIGURE 21.—Bed-form wavelengths versus measures of flow strength.

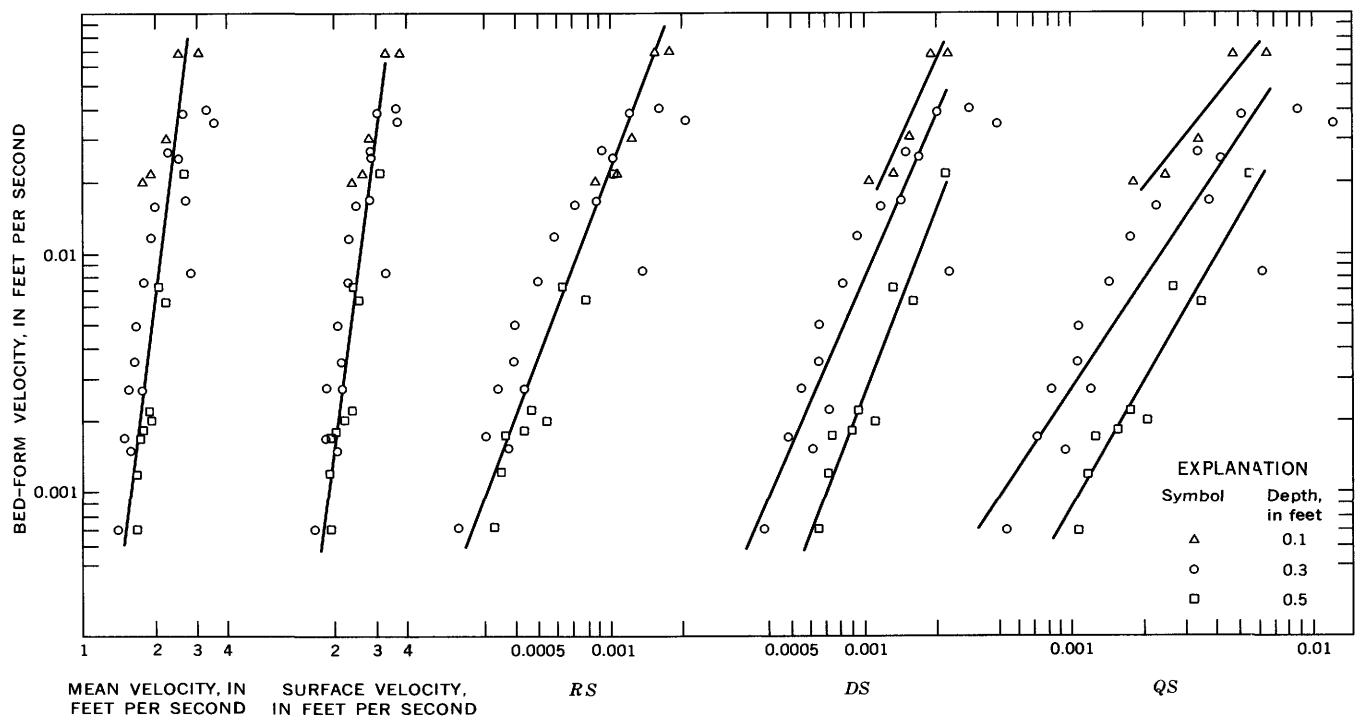


FIGURE 22.—Bed-form velocity versus measures of flow strength.

Their data were obtained in the laboratory in a large recirculating flume. A basic assumption in the derivation of the equation was that the bed forms are triangular from a side view. This was true for only some of

the bed forms of the present experiments. Since triangular bed forms are restricted to a very limited range within the spectrum of bed configurations, it would seem that bedload equations which depend on the

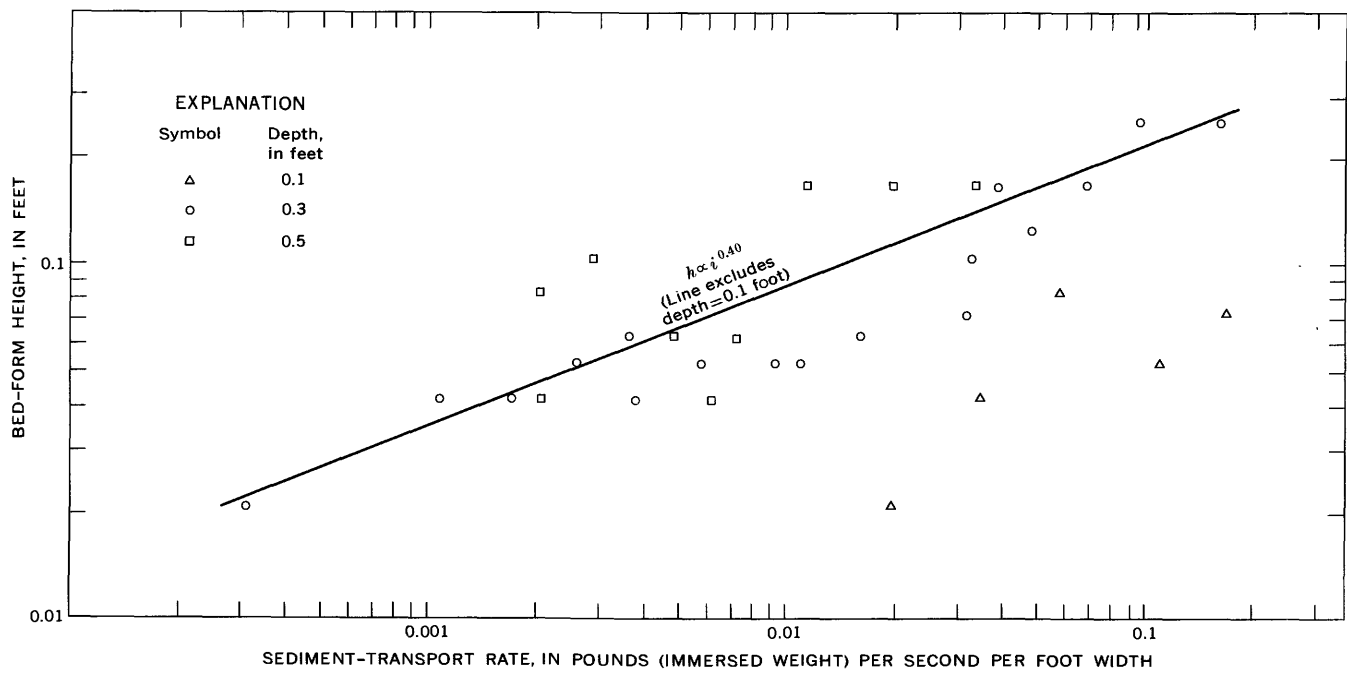


FIGURE 23.—Relation of bed-form height to sediment-transport rate.

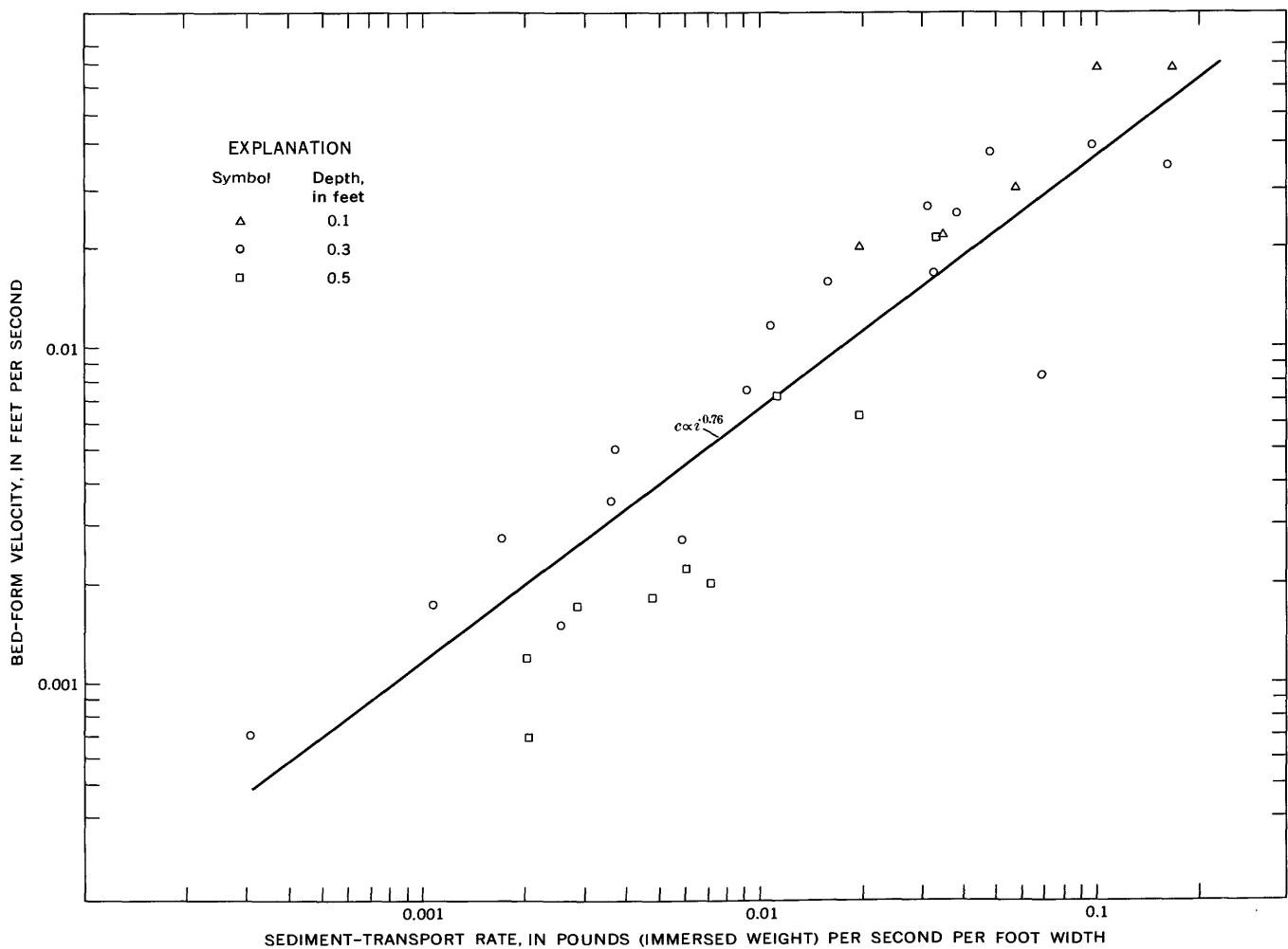


FIGURE 24.—Variation in bed-form velocity with sediment-transport rate.



existence of an ideally shaped bed form will have a rather limited application. The equation is

$$q_b = (1 - \lambda) \frac{ch}{2} + C_1$$

where

$q_b$  = volume rate of sediment transport (ft<sup>3</sup> per sec per ft width),

$\lambda$  = porosity of sand bed,

$c$  = average bed-form velocity (ft per sec),

$h$  = average bed-form height (ft), and

$C_1$  = a constant of integration, considered equal to zero as long as the bed is entirely covered with ripples or dunes.

Volume rate of sediment transport can be changed to weight rate by dividing by the measured unit (specific) weight of the quartz sediment (91.5 lbs per cu ft). This dry weight in turn can be changed to immersed weight, the latter being  $\frac{2.66 - 1.00}{2.66} \times (\text{dry weight}) = 0.624 \times (\text{dry weight})$ . By making these changes and using the measured porosity value of 0.445, the above equation can be reduced to the form

$$i_c = 15.8 ch,$$

where  $i_c$  is the computed sediment-transport rate in pounds (immersed weight) per second per foot of channel width. (The constant  $C_1$  in the original equation can be taken as zero.)

Although the equation was not intended to apply to antidunes, those runs which produced antidunes were included in the present computations merely out of curiosity. A comparison of all the computed versus measured bedloads is shown in figure 25. The amount of point scatter is probably not excessive in view of the uncertainties involved in measuring bed-form heights and rates of travel.

### CONCLUSIONS

For the sediment, flow conditions, and flume of the present study, the following conclusions were drawn:

1. Scatter of points in the sediment-transport diagrams is vastly reduced and existing relations are clarified by keeping water depth constant for a series of runs—that is, by using depth as a third variable.
2. If shear, expressed as  $\gamma RS$ , is used as the measure of flow strength in computing the sediment-transport rate, all the runs can be described by a single curve in which shear is uniquely related to transport rate.

3. Mean velocity, stream power, shear expressed as  $\gamma DS$ , and a regime bed factor are uniquely related to sediment-transport rate only for a constant water depth. Two corollaries of this conclusion are:

- (a) If depth is permitted to vary, the transport rate increases as depth decreases for a given value of any of these four measures of flow strength.
- (b) The critical or threshold flow strength required to initiate sediment transport, as expressed by these four measures, varies with water depth, rather than being uniquely determined by the sediment characteristics and bed slope.

4. The interrelationships between discharge, slope, and sediment-transport rate are uniquely defined only for a constant water depth.

5. If water depth is known, surface velocity is the only other measurement needed to determine the values of all other major variables. Surface velocity may be very useful in this respect because it is so easily measured.

6. The Gilbert-Murphy data for a comparable grain size are in substantial agreement with the present data.

7. A critical water depth somewhere between 0.1 and 0.3 foot exists in the formation of bed forms. At depths shallower than this critical depth, the bed features have distinctly different characteristics than do features formed at greater depths.

### DESCRIPTION OF BED CONFIGURATION, BY RUN

The following are partial descriptions of the bed configurations that formed during each run (numbered). The depth of water for each set of runs is indicated by centerhead.

#### 0.1-foot depth

1. Flat bed.
2. Almost flat bed, although some barely perceptible features were present. These features were meandering scars which began at the wall and curved diagonally outward in a downstream direction; they generally faded out completely in the middle of the channel. Their points of origin alternated systematically from wall to wall. The amplitudes (heights) of the features were on the order of a few grain diameters. There was a downstream distance of about 2 feet from the start of one scar to the start of its neighbor at the opposite wall.
3. Same as previous run.
4. Bed almost flat, although two different types of bed features were faintly discernible:
  - (a) Symmetrical antidunes down much of the flume length but not present near the walls. Crests of these bed forms corresponded to crests of water-surface crests immediately above. Amplitudes of antidunes were too small to measure accurately; wavelength estimated to be 0.5 foot.

NOTE:—These features disappeared as the water was drained from the flume at the completion of the run.

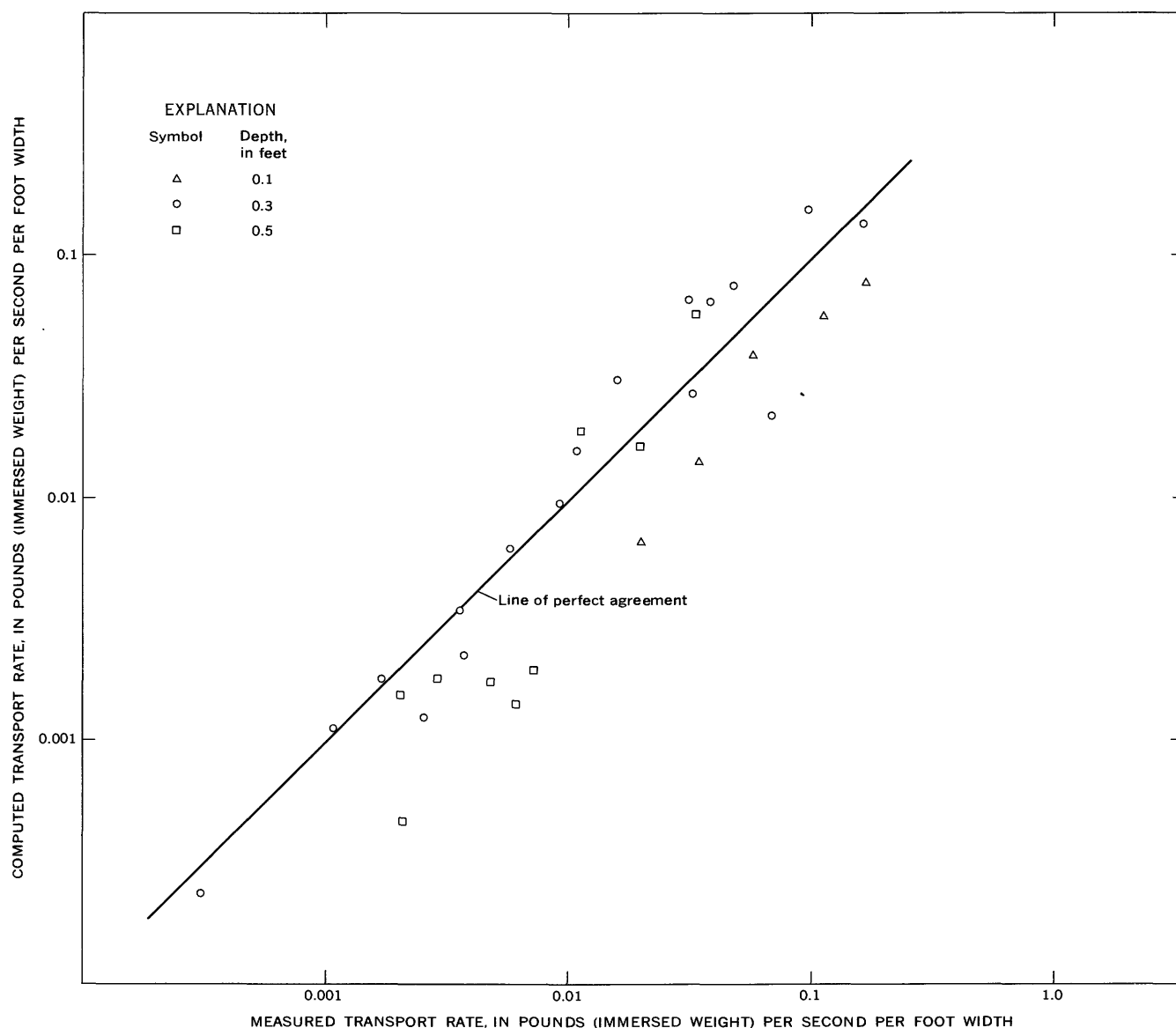


FIGURE 25.—Comparison of computed versus measured transport rates.

- (b) Meandering scars, like those formed in the previous runs, were present, but only downstream. Heights of scars were as much as a quarter of an inch at flume walls but decreased toward the center of the channel, where the bed was almost flat. Downstream distance between successive scar inceptions was about 1 foot.

NOTE:—After the water drained from the flume, features of the latter type were found throughout most of the flume. Rather than fading out in the middle of the channel, each one curved from its point of inception, at a wall, downstream and over to the opposite wall, at which point a similar feature began. Downstream distance between these two inception points averaged 1.5 feet.

5. Rather symmetrical antidunes (crests were directly beneath the crests of the ripply water surface). As the water drained from the flume, these bed forms disappeared, and meandering scars appeared.

6. Symmetrical antidunes like those in the previous run, but formed in two rows in a longitudinal direction rather than in a single row. An alternating pattern existed whereby one sand crest was closer to one flume wall and the next crest downstream was closer to the opposite wall. The distribution of sand crests and troughs was so regular that it resembled a checkerboard pattern. The water surface was correspondingly rippled in two rows, with neighboring crests staggered relative to each other, in a downstream direction. The amplitude of these water-surface waves was higher than that of the bed forms. The distance from one sand crest to the downstream range of its offset neighbor (parallel to flow) was about 0.35 foot.

All these bed features were smoothed out and disappeared as the water drained from the flume.

7. Same as preceding run.
8. Antidunes (sand crests directly beneath water-surface crests) in a single row; moved downstream in groups or trains. A single sand crest sometimes extended across

the channel width but at other times occupied only about 0.4 foot in the middle of the channel. At times the bed forms were almost obliterated (latter phenomenon was possibly more common in the first 10 ft and in the last 10 ft of the flume). All bed features were regularly spaced throughout the flume length. The water surface was ripply but irregular.

9. Mostly flat bed; an occasional train of antidunes generally about 3 feet long but sometimes as much as 10 feet long.

Water surface mostly rather smooth except where ripply above antidunes; inphase relation between water and sand crests, where such crests existed.

#### *0.3-foot depth*

10. Flat bed. Smooth water surface. Very little sediment movement.
11. Almost flat bed; one or two widely spaced bed features (dunes). Water surface smooth.
12. Almost flat bed; an occasional small dune.
13. Dunes, with fronts higher in center of channel than near walls. Wavelengths of dunes increased systematically in downstream direction. When bed-form observations were made, five dunes were present in the flume.
14. Dunes, many of which were poorly defined. Fronts generally perpendicular to flow direction across whole channel width, and higher in channel center than near walls.
15. Dunes. Wavelengths irregularly spaced.
16. Dunes, with fronts normal to flow and wavelengths not consistent in downstream direction.
17. Dunes, irregularly spaced and possibly tending to have longer wave lengths downstream.
18. Dunes, generally with well-defined fronts and perpendicular to flow. Wavelengths not consistent throughout flume.
19. Same as previous run. Wide range of wavelength magnitudes.
20. Same as previous run.
21. Dunes, with crests often curving irregularly across the channel rather than normal to flow. Fronts continually grew higher, receded, and moved downstream at various rates. Wavelengths were longer and more inconsistent in the downstream half of the flume length, but were regularly spaced in the upstream half of the flume.
22. Dunes, with very irregular crests that generally curved from one wall downstream to the opposite wall. Small parts of the dunes were normal to the flow direction near walls. Bed forms and water surface became increasingly rougher downstream. Dune lengths more variable in downstream part of flume.
23. Dunes, with very irregular and poorly defined crests, particularly upstream. Dune heights and wavelengths varying considerably in magnitude. Possible tendency for dune lengths to cluster, so that reaches of short wavelengths alternated with reaches of longer wavelengths.
24. Dunes, very irregular in cross-sectional and top views but rather evenly distributed throughout flume length.
25. Same as previous run. Water surface very rough and irregular.
26. Antidunes, with sand crests directly beneath water-surface crests. Wavelengths rather constant throughout flume length. Bed-form crests more rounded and water surface smoother than in the runs immediately preceding this.

NOTE:—Bed forms were considerably smoothed out after water drained from flume and bore little, if any, resemblance to the features that were present during the run.

27. Antidunes, with very well rounded crests; consistent in wavelength. As water drained, bed forms were considerably smoothed out, and many meandering scars (run 4b) appeared.
28. Antidunes, rather evenly spaced along the flume and rather symmetrical in form from a side view. Crests very well rounded. Water surface consisted of rough waves whose crests were inphase with the dune crests. These water waves were distinctive because they broke on the upstream side of the wave crest or peak.

#### *0.5-foot depth*

29. Dunes, whose fronts were almost normal to flow direction except near flume walls. Water surface smooth.
30. Dunes, irregularly spaced in downstream direction. Water surface rather smooth; very minor undulations.
31. Dunes, with very well defined angular crests that extended completely across flume width, normal to flow. Water surface rather smooth.
32. Dunes, with crests nearly perpendicular to flow from wall to wall. Crestline slightly irregular. Downstream dunes regularly spaced; upstream dunes not as regularly spaced and generally closer together.
33. Dunes, with well-defined crests normal to flow; dunes irregularly spaced relative to one another. Some possible tendencies of clustering of similar dune lengths. Minor undulations in water surface.
34. Dunes, with well-defined angular crests normal to flow direction; not very regularly spaced in downstream direction. Rather smooth water surface, with very minor undulations about 1 foot long.
35. Same as previous run, except less variation in dune lengths.
36. Dunes, with crests sometimes curving downstream from one wall to the other and at other times perpendicular to the flow direction. Possible tendency for clustering of similar dune lengths. Water surface had undulations about 1 inch high and 1 foot long. No discernible relation between water-surface crests and bed-form crests.
37. Dunes, some with crests straight across channel (possibly more common upstream), and others with crests curving downstream from wall to wall (mostly in downstream half of flume). Dunes tended to be regularly spaced along flume. Undulating water surface, with troughs directly over dune crests.

#### REFERENCES

- Brooks, N. H., 1954, Laboratory studies of the mechanics of streams flowing over a movable bed of fine sand: Pasadena, California Inst. Technology Ph. D. thesis, 248 p.
- 1958, Mechanics of streams with movable beds of fine sand: Am. Soc. Civil Engineers Trans., v. 123, p. 526-549.
- Colby, B. R., 1964a, Practical computations of bed-material discharge: Am. Soc. Civil Engineers Proc., v. 90, no. HY2, p. 217-246.
- 1964b, Discharge of sands and mean-velocity relationships in sand-bed streams: U.S. Geol. Survey Prof. Paper 462-A, 47 p.
- Colby, B. R., and Scott, C. H., 1965, Effects of water temperature on the discharge of bed material: U.S. Geol. Survey Prof. Paper 462-G, 25 p.
- Einstein, H. A., 1942, Formulas for the transportation of bed load: Am. Soc. Civil Engineers Trans., no. 107, p. 561-577.

- Gilbert, G. K., 1914, Transportation of debris by running water: U.S. Geol. Survey Prof. Paper 86, 263 p.
- Langbein, W. B., 1964, Geometry of river channels: Am Soc. Civil Engineers Proc., v. 90, no. HY2, p. 301-312.
- Liu, H. K., 1958, *in discussion to "Mechanics of streams with movable beds of fine sand,"* by N. H. Brooks: Am. Soc. Civil Engineers Trans., v. 123, p. 568.
- Simons, D. B., Richardson, E. V., and Nordin, C. F., Jr., 1965a, Sedimentary structures generated by flow in alluvial channels, *in Soc. Econ. Paleontologists and Mineralogists, Primary sedimentary structures and their hydrodynamic interpretation—a symposium*: Soc. Econ. Paleontologists and Mineralogists Spec. Pub. 12, p. 34-52, 253-264.
- 1965b, Bedload equation for ripples and dunes: U.S. Geol. Survey Prof. Paper 462-H, 9 p.
- Sundborg, Å., 1956, The river Klarälven—a study of fluvial processes: Geog. Annaler, v. 38, p. 127-316.
- U.S. Inter-Agency Committee on Water Resources, 1957, Some fundamentals of particle size analysis, *in A study of methods used in measurement and analysis of sediment loads in streams*: Washington, U.S. Govt. Printing Office, Rept. 12, 55 p.
- Vanoni, V. A., and Brooks, N. H., 1957, Laboratory studies of the roughness and suspended load of alluvial streams: California Inst. Technology Sedimentation Lab. Rept. E-68, 121 p.

